The Meteoritical Society

Meteoritics & Planetary Science 1–29 (2017)
doi: 10.1111/maps.12924

Invited Review

Dating very young planetary surfaces from crater statistics: A review of issues and challenges

Jean-Pierre WILLIAMS[1,*], Carolyn H. VAN DER BOGERT[2], Asmin V. PATHARE[3], Gregory G. MICHAEL[4], Michelle R. KIRCHOFF[5], and Harald HIESINGER[2]

[1]Department of Earth, Planetary and Space Sciences, University of California, Los Angeles, California 90095, USA
[2]Institut für Planetologie, Westfälische Wilhelms-Universität Münster, Wilhelm-Klemm-Str. 10, 48149, Münster, Germany
[3]Planetary Science Institute, Tucson, Arizona 85719, USA
[4]Planetary Sciences and Remote Sensing, Institute of Geological Sciences, Freie Universitaet Berlin, Malteser Strasse 74-100, Haus D, Berlin 12249, Germany
[5]Southwest Research Institute, 1050 Walnut Street, Suite 300, Boulder, Colorado 80502, USA
[*]Corresponding author. E-mail: jpierre@mars.ucla.edu

(Received 30 November 2016; revision accepted 25 May 2017)

Abstract–Determining the ages of young planetary surfaces relies on using populations of small, often sub-km diameter impact craters due to the higher frequency at which they form. Smaller craters however can be less reliable for estimating ages as their size-frequency distribution is more susceptible to alteration with debate as to whether they should be used at all. With the current plethora of meter-scale resolution images acquired of the lunar and Martian surfaces, small craters have been widely used to derive model ages to establish the temporal relation of recent geologic events. In this review paper, we discuss the many factors that make smaller craters particularly challenging to use and should be taken into consideration when crater counts are confined to small crater diameters. Establishing confidence in a model age ultimately requires an understanding of the geologic context of the surface being dated as reliability can vary considerably and limitations of the dating technique should be considered in applying ages to any geologic interpretation.

INTRODUCTION

Impact craters currently provide the best mechanism for absolute dating planetary surfaces other than the Earth and locations on the Moon where in situ samples were acquired by the Luna and Apollo missions providing age estimates through radiometric and cosmic-ray exposure age-dating techniques (e.g., Turner 1977; Heiken et al. 1991; Nyquist and Shih 1992; Papike et al. 1998; Snyder et al. 2000; Nyquist et al. 2001). The relative ages of a planetary surface can be established from the observed population of superposed craters; however, the determination of absolute ages requires information on the rate of the accumulation of craters over time. Modeled impact crater chronologies rely on correlating the ages derived from the age-dated lunar samples (e.g., Arvidson et al. 1975; Stöffler and Ryder 2001; Stöffler et al. 2006) to observed crater size-frequency distributions (CSFDs) to anchor the lunar crater chronology and enable systems of crater retention-age models to be developed for the Moon (e.g., Neukum 1983; Neukum et al. 2001) and extrapolated to other inner solar system bodies, such as Mars (Ivanov 2001; Hartmann 2005), Mercury (Fassett et al. 2011), Venus (Herrick et al. 1997), Vesta (Schmedemann et al. 2014), and Ceres (Hiesinger et al. 2016a). This dating technique has been developed over several decades (e.g., Öpik 1960; Shoemaker et al. 1963, 1970; Baldwin 1964; Hartmann 1965, 1966a, 1999, 2005; Greeley and Gault 1970; Neukum and Wise 1976; Crater Analysis Techniques Working Group 1979; Moore et al. 1980; Neukum 1983; Neukum and Ivanov

1994; Hartmann and Neukum 2001; Neukum et al. 2001), and has been recently revisited (Marchi et al. 2009; Le Feuvre and Wieczorek 2011; Hiesinger et al. 2012; Robbins 2014) as more recent image data have become available along with an improved understanding of impactor dynamics and asteroid populations (also see recent review by Fassett [2016] and references therein).

The chronology systems contain two elements: a production function (PF) describing the CSFD shape and the chronology function (CF) relating the accumulated crater density to absolute time. Collectively, these yield a predicted CSFD, or isochron, for a given length of time a surface has been exposed to impact cratering. To apply isochrons based on the lunar chronology system to other solar system objects requires an additional extrapolation that accounts for differences in encounter velocities, surface gravity, and impactor flux (e.g., Ivanov 2001; Hartmann 2005).

Due to the higher frequency at which smaller energy impacts occur, age estimates of very young surfaces or geologic features often require using craters with diameters limited to a range where their production function is less certain and the craters are more sensitive to variation and modification. Various processes preferentially alter crater populations at smaller diameters (e.g., Öpik 1965) resulting in deviations in the CSFD such as: ablation, deceleration, and fragmentation of meteors traversing an atmosphere prior to impacting the surface; secondary and self-secondary cratering; the influence of target properties on crater scaling; and postformation modification of craters through erosion and deposition. Therefore, crater counts limited to small, sub-kilometer crater diameters are at greater risk of yielding an age that may be misinterpreted if the modeled PF has not accounted for the factors that have altered the CSFD within the observed diameter range (Hartmann et al. 1981).

Additionally, ages derived for young surfaces will be sensitive to variations in the impactor flux including episodes of enhanced cratering resulting from the disruption of asteroids as the integration time is limited to the recent past and may not be representative of the longer term average assumed in the modeled chronologies (e.g., Hartman and Hartmann 1968; Hartmann 1970; Bottke et al. 2007; Kirchoff et al. 2013). Additional uncertainties arise as crater identification may be prone to biases at smaller sizes by illumination effects and resolution limits, and limited numbers of craters or confined crater-count areas can introduce statistical uncertainties (Soderblom 1970; Young 1975; Wilcox et al. 2005; Ostrach et al. 2011; Hiesinger et al. 2012; Van der Bogert et al. 2015a, 2015b; Michael et al. 2016).

All of these issues render the modeling of ages using predominately small craters susceptible to error. Yet the need to discriminate very young features is vital to addressing many outstanding questions in planetary science. Given the complicating factors making small craters challenging to use in establishing ages, the question of whether such ages can be determined reliably and confidently within the uncertainty required to be useful in making geologic interpretations is one of utmost importance. In this paper, we review these issues and their potential influence on model age estimates of very young surfaces.

IMPACT RATES

Current Observations

The development of CFs, derived from crater counts correlated with dated lunar samples, has made it possible to assign absolute model ages to unsampled regions of the Moon, and other inner solar system bodies. After an initial rapid decline in cratering early in lunar history, the impact rate has been relatively constant over the last 3 Gyr (e.g., Guinness and Arvidson 1977; Neukum 1983; Neukum et al. 2001), though there is evidence that the cratering rate may have declined by a factor of ~3 during this period (Hartmann et al. 2007; Quantin et al. 2007). A gap in lunar samples with ages ~1–3 Ga, however, limits our understanding of the true nature of the cratering chronology during this period and the resulting large uncertainties in the rate will likely remain unresolved without the future acquisition (or eventual in situ dating) of new samples with such ages. A recent attempt to calibrate an age for Autolycus crater, which would presumably fall within this unrepresented age range, was unsuccessful, likely due to secondary contamination from Aristillus (Hiesinger et al. 2016b). Observations of the present-day impact rate of smaller frequently encountered objects, however, provide a useful comparison to commonly used production and CFs and assess their reliability for dating very young surfaces (Williams et al. 2014a, 2014b; McEwen et al. 2015).

Surveys of objects colliding with the Earth provide estimates of the size-frequency distribution (SFD) and flux of small impactors at 1 AU. These objects generally do not reach the surface as a single body, but deposit energy in the atmosphere that is detectable via optical, seismic, or acoustic/infrasound sensors (Ceplecha et al. 1998). Various surveys are plotted in Fig. 1 normalized to an annual flux. Brown et al. (2002) reported results of bolide detections in the terrestrial atmosphere from 8.5 yr of optical satellite observations operated by the Department of Defense and the Department of Energy.

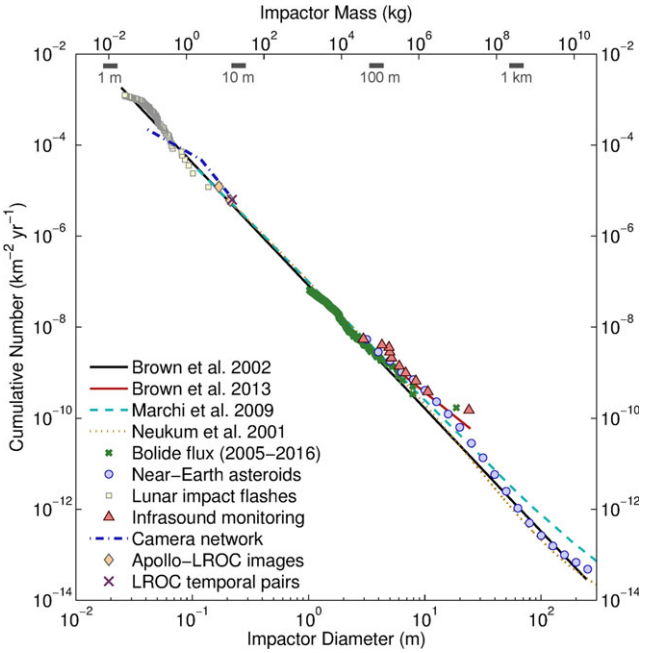

Fig. 1. Estimates of the cumulative population of terrestrial impactors. Black and red solid lines are the power-law fits to the satellite data reported by Brown et al. (2002, 2013), respectively. Dashed cyan curve is the production function of Marchi et al. (2009) and the orange dotted curve is the production function of Neukum et al. (2001). Green 'x' are the latest satellite fireball detections reported by the NASA JPL fireball and bolide reporting website (http://neo.jpl.nasa.gov/fireball/) that includes 390 events from January 1, 2005 to July 7, 2016. Circles are optical surveys of near-Earth asteroids (Harris and D'Abramo 2015) assuming an impact probability of 2×10^{-9} (Brown et al. 2002) and the relation between absolute magnitude and diameter of Bowell et al. (1989) with a mean albedo of 0.14. Squares are lunar impact flashes for events with magnitude 9 or brighter (Suggs et al. 2014). Triangles are bolides detected by global infrasound monitoring (Silber et al. 2009) using the energy-period relation of ReVelle (1997). Blue dash-dot line segments are fireball detection from optical camera network (Halliday et al. 1996). Diamonds are two craters confirmed by LROC images to have formed since Apollo with measureable diameters (Daubar et al. 2011) and the magenta 'x' are the $D \geq 10$ m newly formed craters detected by LROC NAC temporal image pairs (Speyerer et al. 2016). Dark gray bars and labels indicate equivalent lunar crater diameters for impact velocities 10–20 km s^{-1} assuming an impact angle of 45°.

The optical flashes corresponded to objects a few meters in diameters (0.1–10 kiloton equivalent TNT where 1 kiloton = 4.185×10^{12} J) and the power-law fit to the satellite data is plotted in Fig. 1, where we have converted the kinetic energy estimates of the events to diameters assuming a nominal Earth encounter velocity of 20 km s^{-1} and mean projectile density of 2700 kg m^{-3}. The power law is consistent with the Neukum et al. (2001) lunar crater PF for impactors $\lesssim$ a few meters where the Neukum production function (NPF) is scaled to equivalent terrestrial impactors assuming crater scaling parameters appropriate for the lunar regolith (see table 2 of Williams et al. 2014a and Holsapple 1993), a mean impact angle $\pi/4$, a Moon/Earth impact flux ratio 0.725 to account for the gravitational capture cross sectional areas (Ivanov 2006), and a mean Earth/Moon velocity ratio of 1.04 (Le Feuvre and Wieczorek 2011).

An extension of the Brown et al. (2002) survey using nearly 20 yr of bolide data (Brown et al. 2013) found a similar flux; however, the inclusion of the Chelyabinsk event of February 15, 2013 raised the estimated flux of objects ~5 times in the tens of meter size range implying a power-law exponent, or slope on a log-log plot, that is shallower for energies above 1 kT. The latest satellite detections on the NASA JPL fireball and bolide reporting website (http://neo.jpl.nasa.gov/fireball/) include 390 events from January 1, 2005 to July 7, 2016. Chelyabinsk, the largest event, is well above the Brown et al. (2002) power-law estimate for an event of this size given the survey period. Similarly, a 13.67-yr survey of acoustic detections of airbursts by a global network of microbarometers operated by the Air Force Technical Applications Center (AFTAC) (ReVelle 1997; Silber et al. 2009) also indicated a systematically higher flux at these sizes partly as a result of the inclusion of a single large megaton-scale event in August 1963. Silber et al. (2009) note that the source energy estimate techniques have not been calibrated for such high energy events and are extrapolated from lower bolide energy events, possibly explaining the higher flux estimates.

Recent analysis of near-Earth asteroids (NEA), using a computer survey simulation to determine the completion of detections versus size based on the re-detection ratio (D'Abramo et al. 2001), has provided estimates of the SFD of the total population (Harris and D'Abramo 2015). Curvature with peaks and dips is observed in the SFD with a peak at ~10–30 m indicating impact rates are in fact elevated for this size range of impactors (Harris et al. 2015) and could explain the shallower power-law slope implied by the bolide frequency estimates from satellite (Brown et al. 2013) and infrasound detections (Silber et al. 2009) at sizes above a few meters. The curvature is observed in the raw discovery numbers versus size and, thus, is not an artifact of any model bias corrections. Modeling of the impactor flux by Marchi et al. (2009) based on the dynamical models of Bottke et al. (2005a, 2005b) also deviates from the Brown et al. (2002) power law and the NPF at these sizes.

Collisional and dynamical models predict a wavy-shape in the SFD of main belt asteroids as a

consequence of the collisional evolution of the population (Durda et al. 1998; Bottke et al. 2000, 2002, 2005a, 2015; O'Brien and Greenberg 2003, 2005). Wave structure in the model SFDs is generated by asteroids having size-dependent strength. The inflection points occur at approximately the same sizes in the NEA population though the SFD is modified by size-dependent Yarkovsky/YORP-driven migration (Bottke et al. 2006, 2015). Harris and D'Abramo (2015) suggest a transition in internal structure from gravitationally bound "rubble piles" to more cohesive "monolithic" objects may explain the dip in the SFD around 100 m diameter based on rotation statistics, indicating the spin rate of asteroids larger than ~200–300 m is limited by the gravitational spin barrier of ~2.2 h period (e.g., Pravec and Harris 2000). This may explain, at least in part, variations in the power-law slope observed in the impactor and crater populations at these diameters. Impactor estimates do appear to converge however to a common power law at smaller sizes. The slope of the NPF for $D = 250$ m to 1 km is ~ -3.7, but transitions to ~3 below 100 m, which is similar to the Brown et al. (2002) power law and monitoring of lunar impact flashes (Suggs et al. 2014) and fireball detections with camera sky surveys (Halliday et al. 1996). The detection of new lunar craters (Daubar et al. 2011; Speyerer et al. 2016) by the Lunar Reconnaissance Orbiter Camera (LROC) (Robinson et al. 2010) is also consistent with the power law of Brown et al. (2002) in the cm to tens of cm diameter range (Fig. 1).

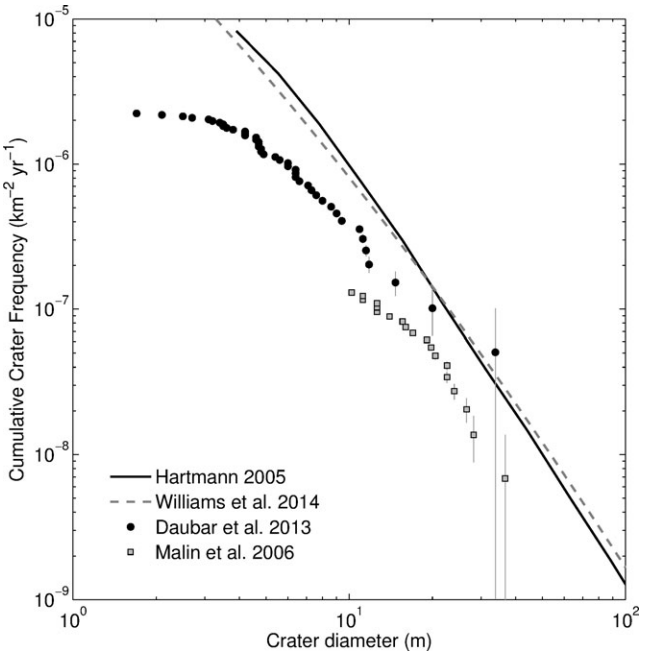

Fig. 2. Fresh craters observed during the MGS mission by MOC (Malin et al. 2006) and the MRO mission by CTX with crater diameters confirmed with targeted HiRISE images (Daubar et al. 2013) along with the crater chronology system of Hartmann (2005) (which may include some unknown fraction of field secondaries) and the predicted SFD for Martian craters derived from the observed terrestrial flux of impactors (Williams et al. 2014a).

The formation of fresh craters on Mars has also been observed by multiple missions (Fig. 2). Initial identification of new craters by the appearance of dark spots in repeat imaging within dust covered regions of Mars by the Mars Orbiter Camera (MOC) (Malin et al. 1992) aboard the Mars Global Surveyor (MGS) mission (Malin et al. 2006) provided a crude estimate of the impactor flux at Mars. Daubar et al. (2013) refined this estimate using fresh craters identified in image data provided by the Mars Reconnaissance Orbiter's Context Camera (CTX) (Malin et al. 2007) and High-Resolution Imaging Science Experiment (HiRISE) (McEwen et al. 2007). The implied flux is generally consistent with the modeled population of meter-scale impactors extrapolated from the observed distribution of known Mars-crossing objects (JeongAhn and Malhotra 2015), and the largest of the new impact craters are consistent with the predicted impact crater formation rate at these sizes by the Martian chronology system of Hartmann (2005). However, fewer craters were observed at smaller sizes resulting in a shallower CSFD slope than the Hartmann production function (HPF). An extrapolation of the terrestrial impactor flux assuming the Brown et al. (2002) power law to equivalent craters on Mars also predicts a steeper CSFD than observed (Williams et al. 2014a). More than half of the fresh craters discovered are crater clusters resulting from fragmentation of the impactors during passage through the atmosphere prior to reaching the Martian surface, indicating disruption of impactors exerts an influence on the resulting CSFD (Hartmann et al. 2017). The HPF accounts for the atmosphere by incorporating an atmospheric model (Popova et al. 2003), although modeling by Ivanov et al. (2014) suggests that the atmosphere may be influencing the smaller diameter impactors to a greater extent than is predicted by this model. Williams et al. (2014a), however, concluded that the atmosphere, including effects of fragmentation, is unlikely to explain the discrepancy in CSFD slopes; recent surveys reported by Hartmann and Daubar (2017) of craters on young, well-preserved surfaces indicate that the atmospheric influence on CSFDs down to ~1–2 m may actually be less than predicted by Popova et al. (2003). Daubar et al. (2016) suggest that more rapid fading of the blast zone albedo patterns around the smaller craters observed in follow-up HiRISE imaging could indicate smaller events may go undiscovered and partly explain the shallower CSFD.

The overlap between the new Martian craters and the chronology system of Hartmann (2005) is reassuring. However, the difference in the CSFD slope remains unexplained, and extrapolated to larger crater sizes results in a higher present-day impact rate than predicted, which suggests that absolute model ages of young surfaces may be overestimated.

Variations in Impact Rates

Chronology models typically make the assumption that the average impact rate has been near-constant at least over the last ~3 Gyr. On shorter time scales, the impact rates may have varied and the present-day impact rate may not necessarily be representative of the longer term average. For example, a survey of ~90 km diameter impact craters on the Moon may indicate extended periods characterized by lulls in the impact rate after 3 Ga with a shorter period (~200 Myr) of elevated impact rates ~1.8 Ga (Kirchoff et al. 2013). This assumes that the flux of small impactors ($\lesssim$1 km) is not correlated with the flux of large impactors ($\gtrsim$5 km), with the small impact flux remaining relatively constant and the large impact flux varying with the breakup of asteroids as modeled in Bottke et al. (2007). Lunar farside rayed craters and terrestrial craters suggest impact rates may have increased late in geologic time (McEwen et al. 1997; Shoemaker 1998) and a periodicity in impact rates has been suggested (e.g., Alvarez and Muller 1984; Shoemaker and Wolfe 1986; Rampino and Caldeira 2015) possibly related to the passage of the Sun through the galactic plane (Matese et al. 1995).

Dating of meteorites and the extraction of extraterrestrial materials in sediments on Earth provide a record of the delivery rate of material over time. The H and L chondrites, ordinary chondrites that make up the majority of meteorite falls, show strong evidence for disruption events of the meteorite parent bodies in the last 500 Ma. Fossilized meteorites in mid-Ordovician limestones reveal a two orders of magnitude increase in the delivery of L chondrite material associated with the breakup of the L chondrite parent body ~466 Ma (Thorslund et al. 1984; Schmitz et al. 1997, 2001; Schmitz 2013) consistent with a large group of L chondrites with gas retention ages ~400–500 Ma (Anders 1964; Keil et al. 1994; Bogard 1995; Haack et al. 1996; Hartmann 2007; Hartmann et al. 2010; Swindle et al. 2014). Cosmic-ray exposure (CRE) ages of chromite grains from the suite of fossil meteorites increase upward in the sediment column indicating many different falls are recorded that originate from a single break-up event reaching Earth at successively later times (Heck et al. 2004). A number of terrestrial impacts also formed in the Late Eocene (~36 Ma) with the two largest craters, Popigai and Chesapeake Bay, forming within a ~10–20 kyr period (Koeberl et al. 1996; Bottomley et al. 1997) with H and L-chondritic chromite grains associated with their ejecta deposits (Schmitz et al. 2015). A peak in CRE ages of meteorites indicate disruption events of both the H and L chondrite parent bodies around the Late Eocene (Wieler and Graf 2001; Kyte et al. 2011), and enrichments of ^{3}He in marine sediments—along with microtektite or krystite beds and iridium anomalies—observed over the corresponding stratigraphic interval have been attributed to an increase in the delivery of extraterrestrial material (Montanari et al. 1993; Farley et al. 1998; Farley 2009; Koeberl 2009; Boschi et al. 2017). It has been suggested that the ^{3}He anomaly, representing a ~2 Myr interval, possibly resulted from an increased flux of impact ejected material from the Moon during this period of time (Fritz et al. 2007) as the upper regolith layer of the Moon contains high (5–50 ppb) ^{3}He-concentrations (Wittenberg et al. 1992; Cocks 2010).

Using the rock abundance signature of the ejecta from Copernican-age lunar craters $D > 5$ km derived from the Diviner instrument on LRO as a proxy for age (Ghent et al. 2014), Mazrouei et al. (2015) and Ghent et al. (2016) find a concentration of craters at all diameters at ~388 Ma that could indicate variations in the impact flux occurred on the Moon. Isotopic ages of lunar impact glass spherules have shown an increase in the frequency of cratering in the last ~500 Ma (Culler et al. 2000; Muller et al. 2001; Levine et al. 2005). However, the lifetimes of spherules are geologically short (Hartmann et al. 2007; Zellner and Delano 2015) as they are prone to breaking into shards and may thus bias the results such that the increase in impact glass spherules during this time may not necessarily be indicative of an increase in the impact flux. The population of most recently formed craters on the Moon, identified by their correlation with patches of anomalously cold nighttime regolith temperatures in Diviner data (Bandfield et al. 2011, 2014), indicates a possible clustering of impact crater formation occurred within the last ~200 ka (Williams et al. 2016a).

How such short-term variations in the impact rate may influence age estimates is unclear, though age estimates on younger surfaces will be more sensitive to such events as the accumulation of craters are integrated over a shorter window of time. The influence could be relatively small, if for example the potential impact cratering spike that occurred in the Late Eocene ~36 Ma resulted in a doubling of the impact rate over a 2 Myr period; a cratered surface would appear only ~5% older than it actually is, much smaller than the

inherent uncertainty in the chronology models. A systematic increase in cratering throughout most of the Copernican period would already be accounted for in the chronology model fits to crater counts during this period. However the age gap in dated lunar samples between ~1–3 Ga precludes any determination as to whether the Eratosthenian had a lower impact rate and thus whether older, intermediate-age surfaces are properly modeled.

ATMOSPHERIC FILTERING

The presence of an atmosphere on a planet complicates the derivation of model ages when constrained to smaller diameter craters. Deceleration, ablation, and fragmentation effects reduce impactor energy as meteors traverse the atmosphere prior to contacting the surface (e.g., Baldwin and Schaeffer 1971; Bronshten 1983; Melosh 1989; Chyba et al. 1993; Popova et al. 2011). Depending on the characteristics of the atmosphere and the range of crater diameters available for dating a surface, the effects of the atmosphere can have a nontrivial influence on the resulting CSFD.

The atmosphere of Venus represents an extreme case in our solar system with a surface pressure of ~92 bars (Fig. 3). Such an atmosphere plays a large role in modifying crater formation (Schultz 1992). Less than 1000 craters have been identified globally with the smallest craters ~1.5 km in diameter (Schaber et al. 1992; Herrick et al. 1997). The atmosphere alters the CSFD up to crater diameters ~30 km (Phillips et al. 1992) where the global CSFD is observed to deviate from a power-law distribution. The low density and broad, near-random dispersal of craters globally provide little constraint on relative timing and duration of formation of surface units (Campbell 1999; Ivanov and Head 2011).

Titan similarly has few craters with an area fraction of craters similar to Venus (Wood et al. 2010; Neish and Lorenz 2012). The atmospheric temperature and pressure of ~93 K and ~1.5 bar measured by the Huygens probe at the surface (Fulchignoni et al. 2005) correspond to an atmospheric surface density ~4 times that of Earth. The lower surface gravity acceleration (1.35 m s^{-2}) also results in an atmosphere that is significantly distended relative to Earth with meteoroids experiencing the initial effects of drag and ablation at much higher relative altitudes (Fig. 3). The models of Zahnle et al. (2003) and Artemieva and Lunine (2005) predict a significant reduction in the formation of craters with diameters <~20 km as the projectiles will be significantly disrupted by the atmosphere. The suppression of small crater formation by the atmosphere and lack of global radar coverage challenges the ability to clearly distinguish ages with more granularity than a global average surface age, with the possible exceptions of Xanadu, which appears to be older and has equatorial dune areas that have lower than average crater densities (Wood et al. 2010).

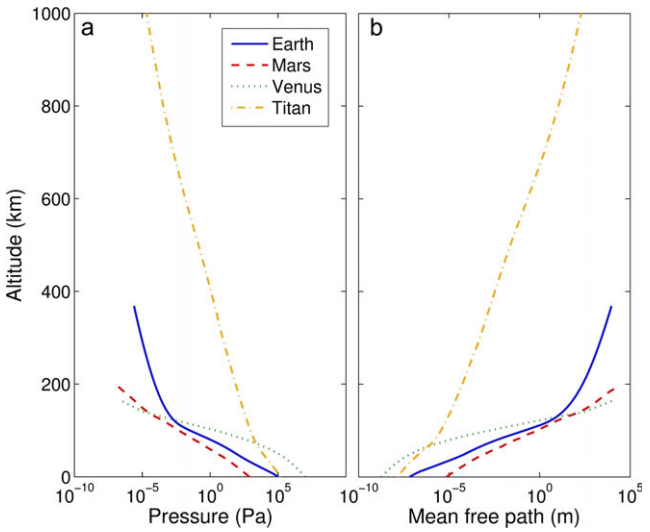

Fig. 3. (a) The pressure and (b) mean free path with altitude above the surface of the atmospheres of Earth, Mars, Venus, and Titan (U.S. Standard Atmosphere, 1976, U.S. Government Printing Office, Washington, D.C., 1976; Seiff and Kirk 1977; Seiff 1983; Yelle et al. 1997).

The atmosphere of Mars by comparison has a more modest influence on crater formation with sub-meter craters capable of forming under current atmospheric conditions (Hörz et al. 1999; Newsom et al. 2015). The magnitude of deceleration and ablation experienced by meteors traversing the atmosphere will depend on the initial velocity and mass of the objects (e.g., Baldwin and Schaeffer 1971; Bronshten 1983; Melosh 1989; Ip 1990; Chyba et al. 1993; Davis 1993; Vasavada et al. 1993; Popova et al. 2000; Artemieva and Shuvalov 2001; Chappelow and Sharpton 2005), with CSFDs becoming increasingly altered by the effects of the Martian atmosphere with decreasing impactor mass starting at crater diameters around a couple hundred meters. Objects with a mass roughly equivalent to or smaller than the mass of the atmospheric column encountered will be significantly decelerated and unable to impact the surface at hypervelocity (typically defined as greater than the sound speed of the target material). This can be approximated by assuming the atmospheric column mass to be $\rho_a HA$ where ρ_a is the surface density of the atmosphere, H is the scale height, and A is the meteor cross sectional area (Williams et al. 2014a). For a nominal Martian atmospheric surface pressure of 6

mbars, this corresponds to impactor diameters of ~9 cm assuming a density of 2700 kg m^{-3}. For comparison, this critical impactor diameter is ~60 m and ~570 m for the Titan and Venus atmospheres respectively and increases to ~170 m for Titan assuming a cometary impactor density of water ice.

The size-dependent reduction in impactor energy by the Martian atmosphere results in a CSFD that increasingly deviates from that expected for an airless body at smaller diameters. The latest iteration of the Martian chronology system by Hartmann (2005) includes the atmospheric entry model of Popova et al. (2003) in an attempt to account for the influence of the current atmosphere on age estimates at the smallest sizes.

The present-day atmospheric conditions on Mars are unlikely to have persisted for more than the past few hundred thousand years (Head et al. 2003; Laskar et al. 2004; Levrard et al. 2004; Haberle et al. 2012). Climate models predict that obliquity-forced changes on the distribution of insolation on Mars' surface result in large-scale variations in atmospheric mass on time scales of 10^5–10^6 yr as a response to changes in partitioning of the CO_2 inventory between the atmosphere and the surface (Ward et al. 1974; Toon et al. 1980; François et al. 1990; Fanale and Salvail 1994; Montmessin 2006). During periods of low obliquity, the atmospheric pressure is expected to drop with the sequestering of CO_2 in the polar caps where surface temperatures are below the sublimation temperature of CO_2 (Leighton and Murray 1966) resulting in "atmospheric collapse" (Haberle et al. 1994; Kreslavsky and Head 2005; Soto et al. 2015). Conversely, periods of high obliquity result in increased annual average insolation at the poles, sublimating CO_2 in the polar caps and regolith, driving up atmospheric surface pressure. The total inventory of CO_2 available to the atmosphere-seasonal cap system is uncertain though buried deposits of CO_2 ice within the south polar layered deposits (SPLD), recently revealed by SHARAD (Shallow Radar), represent a reservoir that would increase the atmospheric mass by up to 80% (5 mbar) if released into the atmosphere at times of high obliquity (Phillips et al. 2011). Kieffer and Zent (1992) estimate the amount of CO_2 absorbed in the regolith could be as much as 70 mbar equivalent. The discovery of sizable iron meteorites by the Opportunity rover has been cited as evidence for a past thicker atmosphere (Beech and Coulson 2010; Chappelow and Sharpton 2006) though Chappelow and Golombek (2010) have found these meteorites could have been decelerated enough in the present-day atmosphere to survive impact under a narrow range of initial entry conditions.

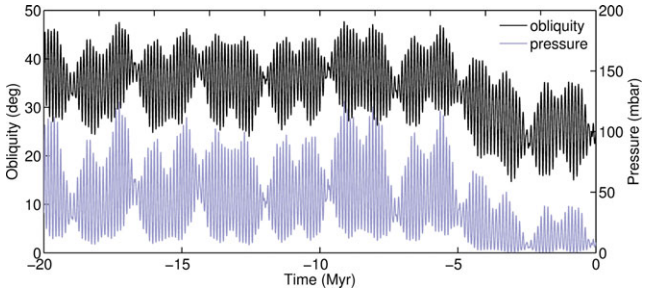

Fig. 4. The obliquity history of Mars from Laskar et al. (2004) and corresponding paleopressure assuming unlimited availability of CO_2 over the last 20 Ma.

A robust prediction of the obliquity history for Mars has been developed for the last 10–20 Ma (Laskar et al. 2004). The obliquity has varied between ~15°–35° during the last 4.5 Myr (Fig. 4) after transitioning from a period of higher mean obliquity (~36°). Prior to the last 20 Ma, deterministic predictions are not possible as the model input parameters become chaotic; however, several candidate obliquity histories over the last 250 Ma produced by Laskar et al. (2004) represent a wide spread of climate options for the Late Amazonian climate history. A general paleopressure history derived using the obliquity history over the last 20 Ma (Fig. 4), estimated from the annual average insolation at the poles and assuming the CO_2 atmosphere is in equilibrium with perennial CO_2 ice deposits (Ward et al. 1974), indicates pressures have been typically higher than present-day. However, peak paleopressures may have been limited by the availability of CO_2, making the paleopressure history uncertain. Given the possible paleopressure history over the last 20 Ma depicted in Fig. 4, a Monte Carlo simulation of crater production assuming the impactor population and encounter velocities described in Williams et al. (2014a), predicts a greater downturn in the CSFD using the time-varying pressure history relative to a constant 6 mbar atmosphere (Fig. 5). While the CSFD of the simulated 20 Ma surface is similar to that predicted using the HPF (Hartmann 2005), the craters for the time-varying pressure history are better fit by a ~5–6 Ma HPF model age for craters $D \lesssim 30$ m. For older surfaces, uncertainty resulting from paleopressure variability becomes greater, particularly when considering small craters.

CRATER FORMATION HETEROGENEITY

Secondary Craters

Primary craters, formed by the direct impact of an asteroid or comet on a planetary surface, can eject

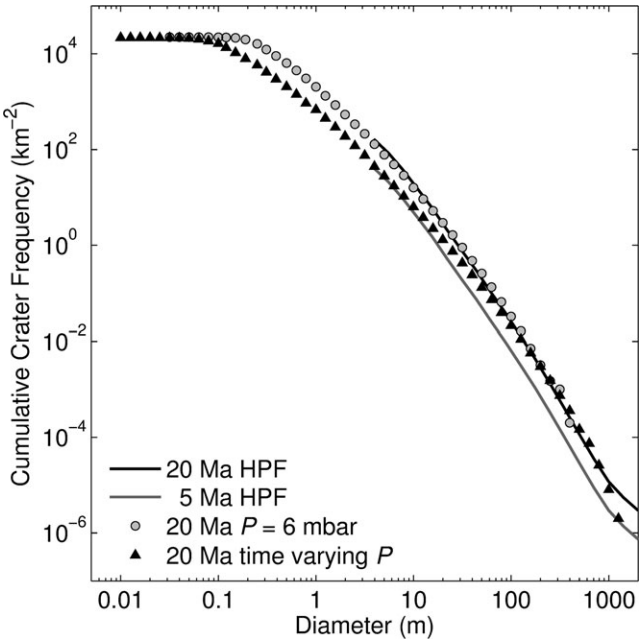

Fig. 5. The CSFDs of a simulated 20 Ma surface on Mars assuming a constant 6 mbar pressure atmosphere (circles) and the time-varying pressure history depicted in Fig. 4 (triangles) and the 20 Ma and 5 Ma model isochrons of Hartmann (2005).

fragments with sufficient energy to form secondary craters when the ejected material re-impacts the surface (see Bierhaus et al. [2017]; for a review). The formation of secondary craters as a consequence of explosive crater formation and its relevance to impact cratering on the Moon was recognized through large-yield chemical and nuclear explosive cratering experiments (Shoemaker 1960; Roberts 1964), the identification of lunar craters associated with rays from Earth-based observations (Fielder 1962; Shoemaker 1962), and the first images of decameter-scale craters from the Ranger VII spacecraft (Kuiper 1965; Miller 1965; Shoemaker 1965), raising concern that craters counts may not reliably be used to determine the flux of impactors on the lunar surface. More recent work concluded that the small crater populations on Mercury (Strom et al. 2008, 2011) and Europa (Bierhaus et al. 2001, 2005) are dominated by secondary craters, and the discovery of $>10^6$ secondaries thought to be generated by the crater Zunil on Mars (McEwen et al. 2005; McEwen and Bierhaus 2006; Preblich et al. 2007) has raised the question of whether this could be the case on Mars as well. It should be noted that a more recently identified crater, Corinto, produced rays and secondaries that crosscut the rays of Zunil, and thus some rays originally attributed to Zunil were likely generated by Corinto (Quantin et al. 2016).

Secondaries represent a geologically instantaneous spike in crater production, in excess of the expected primary crater population. Thus, depending on the fraction of secondary craters, the reliability of an observed crater population as a chronometer will vary, and in the worst case, may be rendered completely useless. Global mapping of primary and secondary craters on Mars by Robbins and Hynek (2014), using the crater database compiled by Robbins and Hynek (2012), shows that secondary craters comprise ~19% of the total population for craters larger than 1 km. This is a conservative estimate as identification of secondaries was somewhat subjective and based on morphologic characteristics; secondaries may have gone unidentified and the distribution is nonuniform with secondary craters outnumbering primary craters in places. At smaller diameters, the proportion of secondary craters that comprise crater populations and their influence on derived model ages remains debated, though comparison between the terrestrial meteoroid flux and small lunar craters on dated surfaces indicates a secondary contamination below 25–50% (Ivanov 2006). This is consistent with crater counts conducted by Neukum et al. (1975) around Bessel crater in Mare Serenitatis that showed the influence of secondary craters on the observed CSFD became negligible at a distance of ~7 crater radii.

Crater counts used to develop the lunar and Martian chronology systems excluded obvious secondary craters, which are generally distinguishable on the basis of their association with rays and aligned chains, herringbone patterns, and clustering near their source craters often orientated toward a primary (Shoemaker 1962; Oberbeck and Morrison 1974; Pike and Wilhelms 1978; Neukum 1983). Distant secondaries with a more random distribution may be indistinguishable from the general crater population. The chronology systems of Hartmann (2005) and Neukum (1983) make no attempt to distinguish these "background" secondary craters with the assumption that the accumulation of both primaries and background secondaries preserves chronometric information (Hartmann 2007).

It was recognized from early high-resolution images of the lunar surface that the slope of the CSFD was steeper for craters with diameters $D < 1$–2 km. This steep branch of the crater distribution was suggested to result from the predominance of secondary craters at these smaller diameters (Shoemaker 1965; Brinkmann 1966). A similar conclusion was made from the global distribution of craters on Mars from Mariner 9 images (Soderblom et al. 1974). The inflection in slope in the distribution, if the result of a crossover point where secondary craters begin to dominate the statistics,

should migrate to larger diameters over time as larger impact craters accumulate and form larger secondary craters (Neukum and Ivanov 1994; Werner et al. 2009). However, this transition in slope is observed to be invariable irrespective of surface age. Ivanov (2006) and Williams et al. (2014a) demonstrated that the observed annual flux of objects impacting the terrestrial atmosphere (Brown et al. 2002) (Fig. 1), scaled to equivalent lunar and Martian craters, can produce a CSFD consistent with the lunar and Martian crater production functions. Small craters ($D < 1$ km) on asteroids such as Gaspra, where secondary craters are thought to be absent due to the very low escape velocity (Cintala et al. 1978; Bierhaus et al. 2012), also display a similarly steep CSFD (Neukum and Ivanov 1994; Chapman et al. 1996; Neukum et al. 2001; Schmedemann et al. 2014), and more recent observations by the Dawn spacecraft (Russell et al. 2012) of two of the youngest terrains on Vesta display a similar CSFD shape (Marchi et al. 2014). The model production functions of Marchi et al. (2009, 2011, 2014) based on modeling of the main belt asteroid population (Bottke et al. 2005a, 2005b) predict a CSFD consistent with the steeper slope at these smaller diameters. Collectively, this indicates the steeper power-law slope at smaller crater diameters is a characteristic of the impactor population, rather than an artifact of secondary cratering.

The outer solar system, however, appears to have a shallow power law slope at smaller crater diameters. Crater counts from Europa (Bierhaus et al. 2001), saturnian satellites (Lissauer et al. 1988; Dones et al. 2009; Kirchoff and Schenk 2010; Bierhaus et al. 2012; Robbins et al. 2015), and Pluto and Charon (Moore et al. 2016; Robbins et al. 2017a) all show shallow-sloped crater populations at diameters <10 km when obvious secondaries and crater clusters are excluded and thus likely reflect a difference in the SFD of the impactor population in the outer solar system (Bierhaus et al. 2005).

Hartmann et al. (2010) examined several young-looking multikilometer impact craters on Mars. These craters displayed systems of rays detectable in Mars Odyssey THEMIS (Christensen et al. 2004) nighttime infrared imagery (Tornabene et al. 2006), and thus were likely the youngest examples of craters of their size as crater rays are relatively ephemeral features. Crater counts by Hartmann et al. (2010) of the superposed craters on the young rayed craters yielded comparable model ages as the expected formation intervals of the host primaries, indicating the multikilometer craters and the superposed decameter-scale craters are linked to a common production function. The relatively young ages of these rayed craters limit the amount of time distant secondary craters could have accumulated, and thus the superposed craters are likely dominated by primary craters implying that the isochrons at small diameter are not dominated by secondary craters.

How the nonrandom formation of secondary craters in space and time might affect model ages, however, remains unclear. Corinto crater (16.95°N, 141.72°E) provides an example of widespread secondary crater formation in the volcanic plains of Elysium Planitia. Located south of Elysium Mons, Corinto has a diameter of 13.8 km and displays dramatic rays in the nighttime THEMIS imagery (McEwen et al. 2010; Ong et al. 2011; Bloom et al. 2014; Golombek et al. 2014a) as ejected material altered the thermophysical properties of the Martian surface (Fig. 6). Isolated ray segments can be identified over 2000 km distance from the primary crater (Bloom et al. 2014). The distant rays formed by Corinto contain concentrations of millions of secondary craters. If a Corinto-size crater is forming on Mars every few Myr with secondary craters-extending to at least 2000 km, any location on Mars has the potential to be impacted by secondary crater forming material within the last 20 Myr. On the Moon, an area of ponded deposits and rocky material within the otherwise nominal lunar highlands terrain may be the result of a concentration of material at the antipode of the 86 km diameter Tycho crater (Artemieva 2013; Jögi and Paige 2015; Bandfield et al. 2016; Robinson et al. 2016). If this material originated from Tycho, it indicates debris from Tycho had the potential to impact the lunar surface globally. The formation of an 18.8 m crater identified with before and after LROC images formed secondary impacts expressed as dark splotches up to 30 km away, indicating even small impacts can modify the lunar surface with ejected material over distances significantly farther than the primary ejecta blanket (Robinson et al. 2015).

The distinct clusters of craters that form rays can generally be identified and excluded from crater counts, as has been done in the development of the production functions. However, outside of the rays, the identification of secondary craters may be ambiguous, especially as any thermal or photometric signature of secondary craters fades with time. Quantin et al. (2016) performed a detailed examination of the secondary crater population around the young rayed Martian crater Gratteri (17.7°S, 199.9°E), a $D = 6.9$ km crater in the Memnonia Fossae region with an estimated age 1–20 Ma. They concluded from their survey that the density of secondary craters outside of rays was low enough that preexisting craters would dominate any surface older than a few percent of Martian history and have minimal influence on crater chronometry. Quantin et al. (2016) and Hartmann and Daubar (2017) point

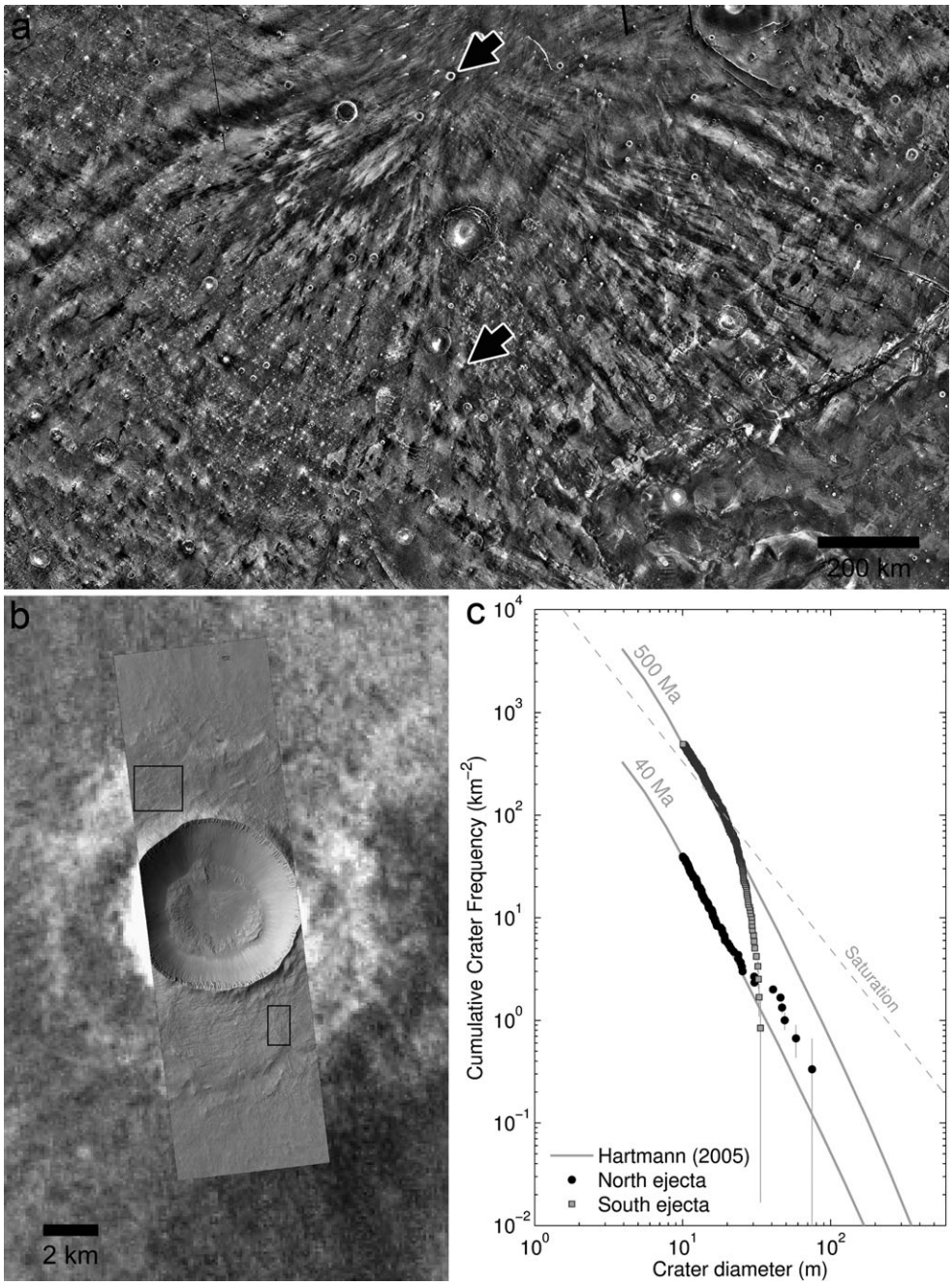

Fig. 6. a) THEMIS IR nighttime 100 m resolution mosaic of region south of Elysium Mons displaying rays from Corinto crater (upper arrow). Lower arrow is location of crater in (b). b) An unnamed crater (D = 6 km) that predates the formation of Corinto crater. Boxes show locations of crater counts using HiRISE image PSP_007659_1885 on the north and south ejecta. A ray segment from Corinto formed on the southern margin of the crater corresponding to the dark area in the background nighttime THEMIS image. c) Crater size-frequency distributions for $D \geq 10$ m for the two regions in (b) with the 40 and 500 Ma model isochrons from Hartmann (2005) and the crater saturation equilibrium function of Hartmann (1984).

out that if Zunil-size impacts large enough to generate global-scale showers of secondary impact craters form every ~1 Myr, then surfaces older than ~20 Ma would contain enough overlapping secondaries to become randomized while surfaces younger than ~0.5 Ma will likely not have experienced global showers of small secondary craters. Surfaces with intermediate ages, however, will be particularly vulnerable to the nonrandom formation rate of secondary craters. An unnamed crater (8.2°N, 142.0°E) in Elysium Planitia

illustrates this possibility as the emplacement of secondary craters from Corinto on the ejecta is heterogeneous and, where secondary craters appear to dominate, obfuscates chronometric information (Fig. 6).

Secondary craters do not just affect surfaces far from their source craters. In fact, they also form on the ejecta blankets of the primary craters themselves. Shoemaker et al. (1968) documented a higher crater density on the Tycho crater ejecta blanket versus the impact melt deposits, and suggested that this density contrast might occur due to the formation of self-secondary craters on the ejecta blanket. They drew a parallel to the formation of self-secondary craters on the debris ejected during the Sedan nuclear test, where secondaries formed just outside the rim of the nuclear crater. Variations in terrain properties appear to be partially responsible for the difference in crater densities between the ejecta blanket and impact melt units (see Discussion below). Nevertheless, populations of candidate self-secondary craters are apparent, and are thought to cause highly variable crater densities even across different parts of the ejecta blanket (Plescia and Robinson 2015; Zanetti et al. 2017), for example at the lunar craters Giordano Bruno (22 km; 36°N, 103°E) (Plescia et al. 2010; Xiao and Strom 2012; Williams et al. 2014b, 2016b), Cone (340 m; 3.62°S, 17.43°W) (Plescia and Robinson 2011; Hiesinger et al. 2015), North Ray (950 m; 8.82°S, 15.48°E) (Plescia and Robinson 2011; Hiesinger et al. 2012), Tycho (86 km; 43.31°S, 11.36°W) (Hiesinger et al. 2012; Zanetti et al. 2017), and Aristarchus (40 km; 23.7°N, 47.4°W) (Zanetti et al. 2017). Craters with unusual morphologies on the impact melt ponds may also represent self-secondaries that formed while impact melt was still molten or viscous (Plescia 2012, 2015).

Figure 7 shows examples of self-secondary craters on the ejecta of Giordano Bruno where it appears that some impact melts were emplaced after the formation of the craters on the ejecta blanket, as evidenced by melt that partially buries and infills a population of circular, rimmed depressions. These depressions therefore must have formed prior to emplacement of the melt following deposition of the clastic ejecta. Mapping of craters on the ejecta of Martian crater Tooting also reveals possible self-secondary craters with anomalously high densities of craters near portions of the southern rim, with the largest craters containing ponded material (Boyce and Mouginis-Mark 2015). Similarly, crater density differences observed at Hokusai crater on Mercury indicate a population of self-secondary craters that appears to predate the formation of melt pools on the crater floor (Xiao et al. 2016) and a fresh looking rayed crater on Rhea (Inktomi) has a heterogeneous distribution of superposed small craters on its floor and ejecta proposed to be evidence for self-secondaries as another source (younger, large crater) is not obvious (Schenk et al. 2017).

In addition to traditional and self-secondaries, the outer solar system (particularly the Saturn system) also experiences so-called "sesquinaries" (Dobrovolskis and Lissauer 2004; Zahnle et al. 2008; Bierhaus et al. 2012). Sesquinary craters are produced by primary crater ejecta that is traveling fast enough to escape the satellite. This debris orbits the planet for a short time and then impacts a satellite—most often the originating one. These craters will likely not form in a clustered pattern, but be spread across the surface sometimes having hemispherical concentrations (Alvarellos et al. 2005, 2017). They are generally as unrecognizable as distant secondaries in the inner solar system and influence the crater chronology in much the same way since they do not have a known formation rate.

Target Properties

Differences between cratering mechanics for differently sized craters can also influence CSFDs. Smaller craters form in a strength-scaling regime, where the final crater is affected by the projectile parameters, as well as the target properties. In contrast, larger crater dimensions are controlled by the planetary gravity field as excavation by larger impacts result in higher lithostatic stresses (Holsapple 1993; Neukum and Ivanov 1994). For craters with diameters in the strength-scaling regime, density, strength, porosity, and other target properties affect the final diameter of an impact crater (e.g., Chapman et al. 1970; Young 1975; Schultz et al. 1977; Holsapple and Schmidt 1982; Melosh 1989; Holsapple 1993; Ivanov 2006, 2008; Ivanov and Hartmann 2007; Wünnemann et al. 2010; Housen and Holsapple 2011; Le Feuvre and Wieczorek 2011). For example, targets with higher coefficients of friction, more porosity, and larger cohesive strength will produce smaller craters than targets with the opposite properties (e.g., Wünnemann et al. 2010; Housen and Holsapple 2011). The differences in crater diameter can be great enough to cause age discrepancies between the CSFD measured on coeval surfaces with differing physical properties. For example, some lava flows exhibit two different surface types: denser smooth polygonally patterned areas and rough areas of broken platy material with lower bulk density (Iceland: Keszthelyi et al. 2004; Hawaii: Hamilton et al. 2015). Young Martian lava flows exhibiting these two surface textures had been postulated to have different ages based on their CSFDs (Murray et al. 2005; Page et al. 2009). However, Dundas et al. (2010) showed, using

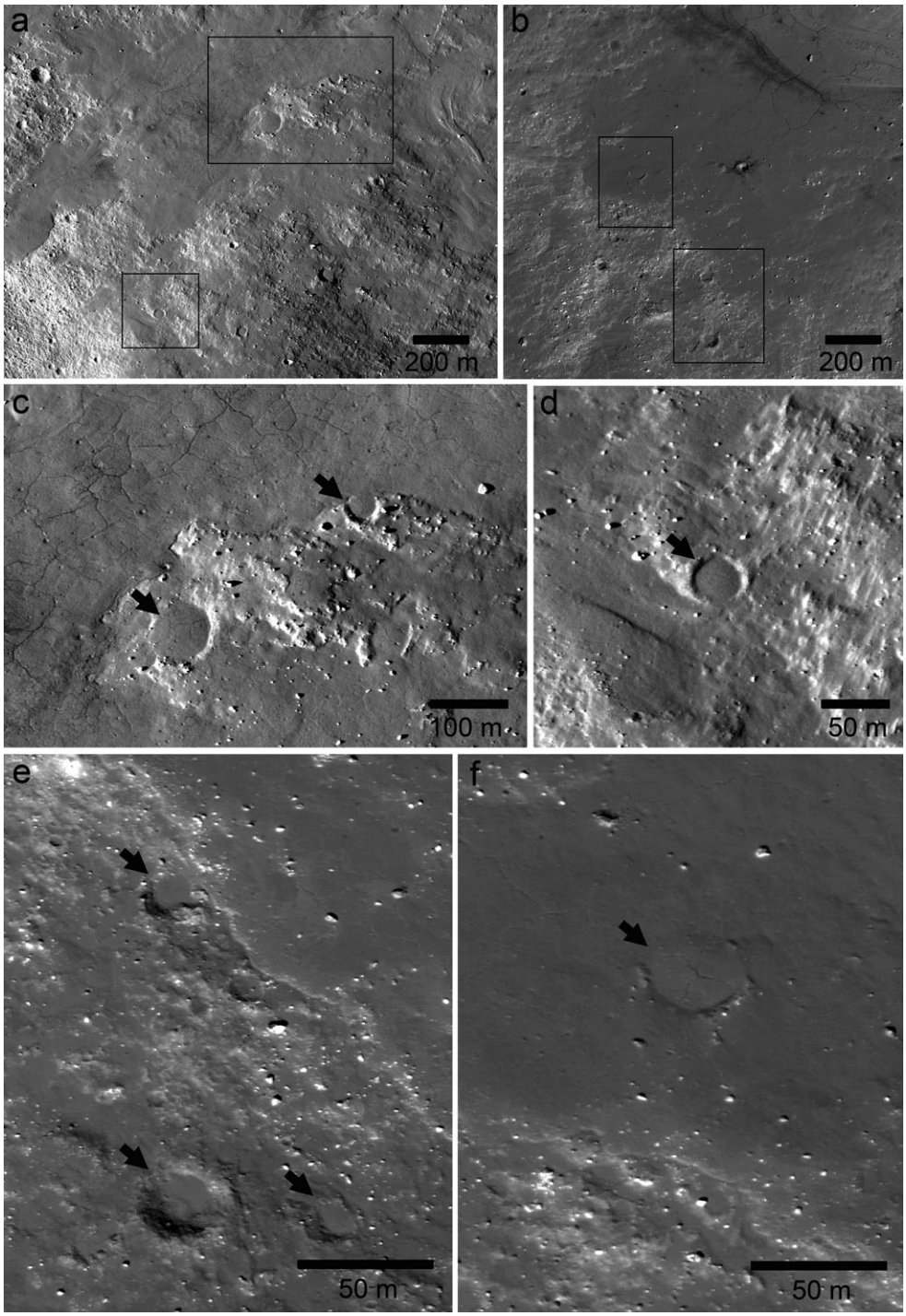

Fig. 7. Impact melt deposits near the south rim of lunar crater Giordano Bruno. a) Portion of LROC NA image M134509592R with boxes showing locations of (c) and (d). b) Portion of LROC NA image M139225065R with boxes showing locations of (e) and (f). c–f) Circular depressions partially buried and infilled by impact melt deposits (black arrows).

pi-scaling calculations and comparisons with terrestrial lava flows, that target property contrasts between the two types could explain final diameter differences for craters with diameters <100 m rather than a real age difference. For Mars, target property effects could also cause there to be lower crater densities on fine-layered deposits, or possibly affect CSFDs on polar-layered deposits, glacial deposits, and frozen ground (Dundas et al. 2010). They also warn that estimates of the current impact rate on Mars may be affected by the

crater diameters measured from recently formed craters, which are found predominately on dusty surfaces. If those surfaces have properties that enlarge of reduce the final crater diameter, estimates of Martian crater production would be either over- or underestimated, respectively.

Similarly, Van der Bogert et al. (2017) reinvestigated age discrepancies between impact melt and ejecta units at Copernican lunar craters. Apollo-era studies of the crater distributions at Tycho, Copernicus, and Aristarchus craters indicated that the impact ejecta deposits were relatively older than smooth deposits associated with the craters, which were thought either to be impact melt or younger volcanics (e.g., Hartmann 1968; Shoemaker et al. 1968; Strom and Fielder 1968a, 1968b). Recently, workers have applied the Neukum et al. (2001) PF/CF to determine model ages for these units, and found statistically significant age differences (e.g., Van der Bogert et al. 2010, 2017; Ashley et al. 2012; Hiesinger et al. 2012; Zanetti et al. 2012). Developments in understanding of the formation and emplacement of impact deposits, as well as the difficulty of producing impact-related volcanism (Ivanov and Melosh 2003), indicate that the "smooth deposits" described in the 1960s are impact melt units, such that a real age difference between the ejecta and melt units is unlikely to be measureable at the resolution of the CSFD technique. Thus, Van der Bogert et al. (2017) investigated whether target property contrasts between impact melt and ejecta could be responsible for the age discrepancy (1) by measuring the CSFD of craters on the largest known impact melt deposit on the Moon—the King crater melt pond (after Schultz and Spencer 1979) (Fig. 8), and (2) via pi-group scaling calculations similar to those by Dundas et al. (2010) for theoretical lunar targets. The resulting CSFD for the King crater melt pond exhibits an age consistent with impact melt units at crater diameters smaller than 255 m (in the strength-scaling regime), whereas it has an age consistent with the ejecta units at crater diameters larger than 310 m (where gravity-scaling starts to play a role) (Van der Bogert et al. 2017) (Fig. 8). This indicates that the discrepancies in the crater sizes are most likely controlled by target property effects. The pi-group scaling calculations also illustrate, as Dundas et al. (2010) showed for Martian lava flows, that different target materials yield craters with significantly different final crater diameters, and that these differences are likely enough to explain the apparent age differences (Van der Bogert et al. 2017) (Fig. 9).

In fact, the slopes of the CSFDs may also be affected by target property effects (Marchi et al. 2011; Kirchoff et al. 2015; Van der Bogert et al. 2017). The

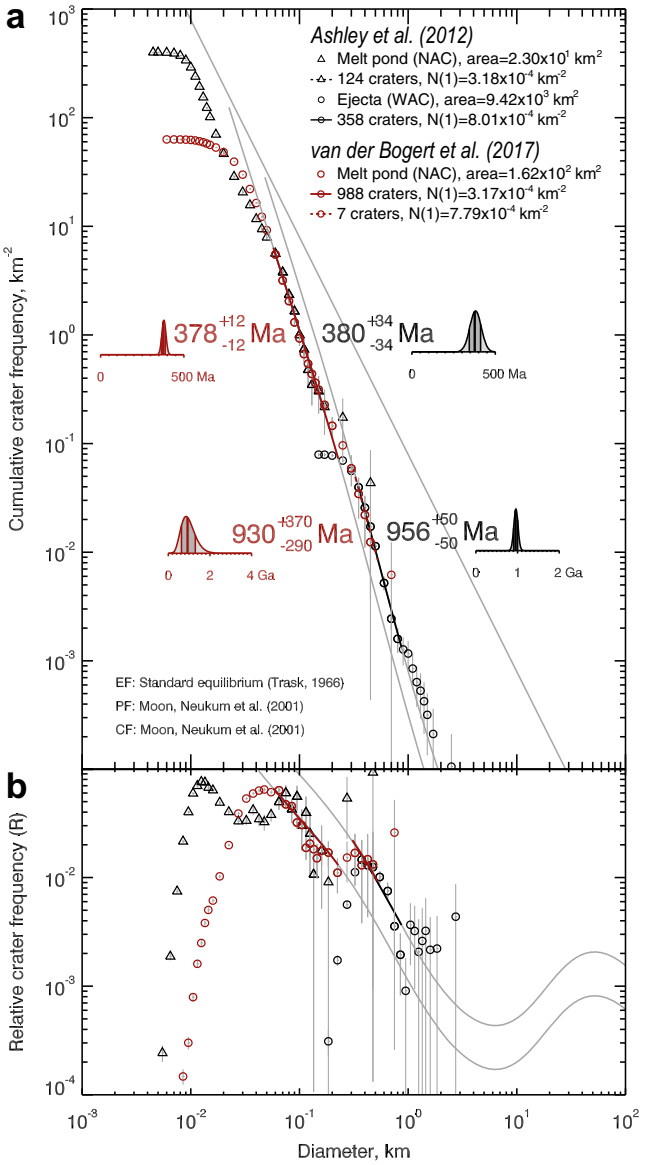

Fig. 8. CSFDs in cumulative (a) and relative (b) plots for King crater using data from Ashley et al. (2012) (black triangles and circles), and a CSFD from Van der Bogert et al. (2017) for a larger portion of the King crater impact melt pond (red circles). Absolute model ages determined using Poisson timing analysis show that both old and young apparent ages can be measured on a single impact melt unit (red), thus supporting the role of target property effects on crater diameters in the strength-scaling regime (<~300 m on the Moon).

implications for the steepening and/or shallowing and shifting of CSFDs due to target property effects are (1) steeper/shallower CSFDs may be difficult to fit with a PF, thereby complicating derivation of model ages, and (2) determination of model ages for small craters from distributions that can be fit with the PF should be

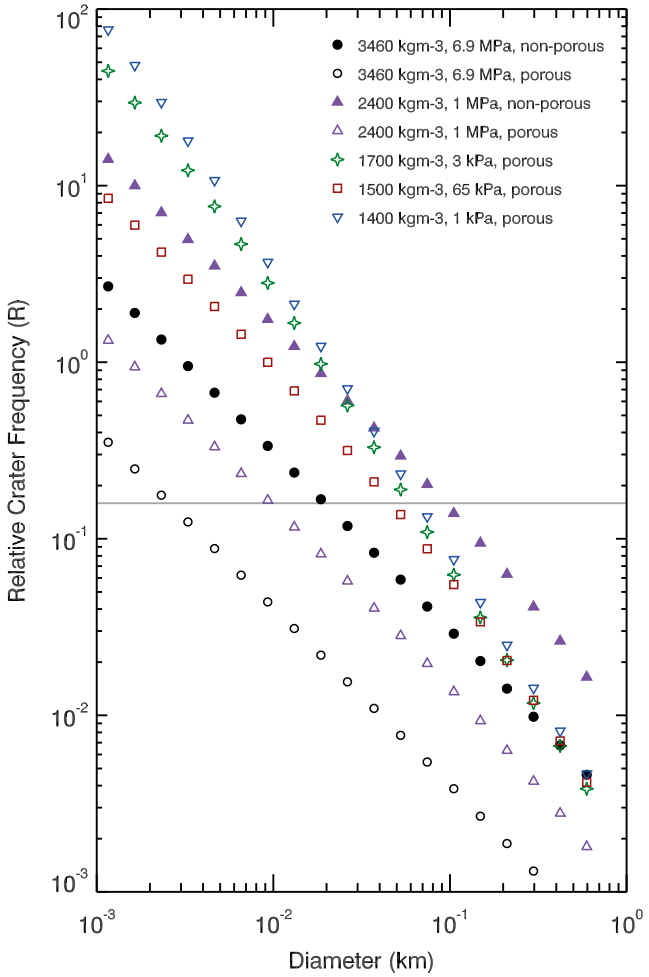

Fig. 9. Relative crater frequency plot of CSFDs generated via pi-group scaling calculations of final crater diameters for different theoretical lunar targets using identical impactor parameters. The gray line represents the standard lunar equilibrium (slope −2; Trask 1966).

interpreted with consideration of the type of target being dated and for the types of surfaces used to construct the PF itself. The Neukum et al. (2001) PF at sub-km diameters was generated largely from CSFD measurements on the continuous ejecta blankets of Copernican-age craters (Neukum 1983; Neukum and Ivanov 1994) and the lunar CF was calibrated using the craters on the ejecta blankets of Copernicus, Tycho, North Ray, and Cone craters. As a result, Copernican surfaces with properties unlike those of ejecta blankets give model ages requiring additional interpretation. For example, ages determined for Copernican-aged irregular mare patches (IMPs) (Braden et al. 2014) may be affected by their presumably nonejecta-like target properties, perhaps enough to affect their apparent absolute model age (Qiao et al. 2017).

CRATER MODIFICATION

General Theory

Small craters can undergo surface modification due to a variety of mechanisms, such as eolian erosion and dust deposition (Öpik 1965, 1966; Hartmann et al. 1981; Hartmann and Neukum 2001; Hartmann 2005) and diffusional creep driven by subsequent impact bombardment (Ross 1968; Soderblom 1970; Lissauer et al. 1988; Fassett and Thomson 2014). Howard (2004) simulated several crater modification processes, including decrescence (uniform erosion), accrescence (uniform deposition), and nonlinear eolian sedimentation (which combines erosion of crater rims with net deposition within crater cavities). Both decrescence and accrescence occur normally to the surface: $dz/dt = (1/\cos\theta) * dn/dt$ (Howard 2004), where dz/dt is the rate of vertical elevation change, θ is the surface slope, and dn/dt is the rate of uniform erosion or deposition (note that, without the slope dependence, the relative surface shape would be unchanged). Such depth-dependent vertical resurfacing processes produce an equilibrium between crater formation and obliteration, resulting in the modification of a cumulative CSFD production function with a slope of $-b$ to an equilibrium function with a slope of $-(b - 1)$, thereby replacing isochron-derived formation ages with resurfacing times (Öpik 1965; Chapman et al. 1969; Hartmann 1971; Herkenhoff and Plaut 2000).

Craters undergoing decrescence exhibit steeper inner rims and smoother floors due to backwasting; in contrast, accrescence produces craters with more rounded rims and negative conical interiors, reminiscent of craters beneath the Martian mid-latitude mantle deposits (Howard 2004). Since uniform dust deposition does not produce a pattern consistent with accrescence (due to the slope dependence of capture), Howard and Craddock (1998) modeled eolian modification as a nonlinear function of the extent of relative surface exposure. Such nonlinear eolian sedimentation results in parabolic crater floors (upon which smaller craters have been eradicated) and crater rims that remain exposed (Forsberg-Taylor et al. 2004; Howard 2004).

Mars

The most comprehensive assessment of recent small crater modification at low latitudes was conducted by Golombek et al. (2014b), who cataloged ~100 craters along the Opportunity rover's traverse in Meridian Planum. Golombek et al. (2014b) identified six classes of crater degradation (dated using the Hartmann [2005]

isochrons), ranging from fresh Class 1 craters <200 kyr old with sharp rims, bowl shapes, and blocky ejecta to heavily eroded Class 6 craters up to 20 Myr old that are rimless shallow depressions lacking ejecta. Their observations indicate a rapid decrease in erosion rate from ~1 m Myr^{-1} for craters <1 Ma to <0.1 m Myr^{-1} for craters 10–20 Ma, which Golombek et al. (2014b) showed is consistent with a slope-dependent topographic diffusion (i.e., nonlinear eolian sedimentation) model with a diffusivity (quantifying material erodibility and erosional vigor) of ~10^{-6} m^2 yr^{-1}. Interestingly, these recent Meridiani erosion rates are 1–2 orders of magnitude faster than those derived for 80–400 Ma by Golombek et al. (2006) from both degradation of larger craters in Meridiani and the concentration of blueberry surface lags, which suggests that present-day Mars is likely undergoing a short-term peak in the efficacy of eolian erosion (Golombek et al. 2014b).

Crater modification rates at higher latitudes are even more rapid. For example, Korteniemi and Kreslavsky (2013) systematically surveyed D = 5–50 m craters in patterned ground between 50–70°N, and found evidence for "surprisingly young" crater retention surface ages in the northern portion of their study, ranging from thousands to just hundreds of years. They attributed these fast crater obliteration timescales to repeated deposition and sublimation of an ice-rich meter-thick mantle that must be occurring during Mars' present-day spin/orbit configuration. Similarly, Landis et al. (2016) revisited crater modification within the north polar layered deposits (NPLD), and concluded that water ice deposition rates are rapid enough to completely infill 100-m diameter craters on time scales of centuries.

The Moon

Basilevsky (1976) characterized the morphological evolution of small lunar craters, identifying five different crater classes based primarily on the depth/diameter (d/D) ratio and the steepness of inner crater wall slopes (which decreases over time due to downslope movement by landslides and avalanches; Basilevsky et al. 2014). Based on this morphological classification, Basilevsky (1976) not only derived diameter-dependent total lifetimes of T (Myr) = 2.5 * D (m) for D < 160 m craters, but also estimated the fraction of time that craters would persist in each of the five evolutionary stages. Basilevsky and Head (2012) utilized this fresh crater classification system to infer ages of 5–10 Ma for fresh D > 20 m craters (some of which were still relatively steep) superposed on the ejecta of Giordana Bruno. More recent models of terrain diffusion rates (Fassett and Thomson 2014; Minton and Fassett 2016) also predict substantially shorter degradation times of smaller craters relative to larger craters. Mahanti et al. (2016) found using digital terrain models derived from LROC stereo observations that small lunar craters typically became unrecognizable when their depth was reduced by 80%, suggesting an upper limit of ~100 Myr for the survival time of craters with diameters 50 m or smaller consistent with Basilevsky (1976). The degradation rate at Taurus Littrow is also found to be significantly faster compared to the Cayley formation suggesting crater degradation rates can vary locally (Mahanti et al. 2016). The accelerated degradation rate in Tarrus Littrow may result from the unconsolidated nature of the thick pyroclastic dark mantling deposits in the area in contrast with the typical layered mare basalts nearby (Lucchitta and Sanchez 1975; Van der Bogert et al. 2016).

Daubar et al. (2014) also studied the morphology of small fresh craters, on both Mars and the Moon. Whereas Martian craters that impacted in the last 20 yr exhibit a mean d/D of 0.23—in accordance with the typical value of d/D ~ 0.2 observed for simple primary lunar craters (e.g., Pike 1974, 1977)—Daubar et al. (2014) measured a much lower average d/D = 0.1 for 500+ random fresh small craters at similar diameters on the Moon. Hence, Daubar et al. (2014) concluded that most of the lunar craters they studied are either unrecognized secondaries or primary craters degraded via steep slope modification, which as noted by Basilevsky et al. (2014) is expected to be a much faster process than infilling by ejecta from near and distant meteoritic impacts.

Effect of Resurfacing on Crater Counts

Resurfacing in general will preferentially remove smaller craters in a population as these craters have less topographic expression (Öpik 1965, 1966). Such size-dependent processes will alter the CSFD. An ongoing, long-term diameter-dependent rate of crater removal results in a CSFD that departs from the crater production function with a shallower slope at smaller diameters (e.g., Hartmann 1971; Neukum 1983; Smith et al. 2008; Newsom et al. 2015; Kneissl et al. 2016). However, an episodic resurfacing event may only partially reset the crater population with the larger diameter craters remaining visible: if such resurfacing goes unrecognized, the reduction in observed craters can erroneously be interpreted as a younger formation age, rather than the age of the resurfacing event, especially if counts are limited to a small range of diameters (Neukum and Horn 1976; Hiesinger et al. 2002; Hartmann et al. 2008; Platz et al.

2010, 2013). The interpretation of the model ages therefore may not be straightforward and may represent a steady state between production and removal of craters (Öpik 1965, 1966), or a diminishing sequence of resurfacing processes, thereby providing a retention age regulated by the destruction rate instead of a surface formation age (Chapman and Jones 1977; Smith et al. 2008; Michael 2013; Fassett 2016; Kite and Mayer 2017).

STATISTICAL AND OBSERVATIONAL BIASES

Limited Numbers of Craters

Established approaches to dating planetary surfaces through the analysis of a superposed crater population rely on the technique of binning the measured crater diameters, and attempting to use the thus divided data to resolve the characteristic shape and density of the accumulating crater population (Hartmann 1966b; Crater Analysis Techniques Working Group 1979; Neukum 1983). The method has seen numerous fruitful applications (see listing of predictive successes in recent review by Fassett 2016), but has always required caution when the number of observed craters is low.

Where we have a large sample of craters, we may be confident that the binned diameters reflect the accumulating population, and expect that the choice of binning has minimal influence on the result. With very few craters, this expectation breaks down, and it no longer makes sense to attempt to resolve a distribution shape from a set of bins containing mostly zero or one diameters. Thus, it is often asked "How many craters are required to make a valid age estimate?"

A better formulated question, however, is "How long does it take for the observed configuration of n craters to form?" If we expect craters of given sizes to form at known rates, Poisson statistics give the probability of occurrence of the observed configuration after any time t (Herkenhoff and Plaut 2000). If we evaluate the probability for all values of t, we have a relative probability function that fully describes the possible age of the surface (Michael et al. 2016). With this approach, we are no longer attempting to resolve the distribution from the observation. Instead, the chronology model describes the distribution, and the Poisson statistics determine the time-resolved probability of the given observation within the model. There is no minimum number of craters for this procedure: even a surface with no superposed crater carries time information. The Poisson statistics can inform, in a probabilistic sense, how young an uncratered surface may be. How many craters are required to make a valid age estimate? None.

Limited Count Areas

One challenge associated with dating young surfaces is that recent geological activity tends to be very spatially limited. As a result, the numbers and sizes of craters available for statistics are also limited. In a test of age determinations of small 4 km^2 areas within a 100 km^2 large reference area on the Moon, Pasckert et al. (2015) showed that the majority of the small count areas gave model ages that are consistent with those of the larger area, but with lower accuracy. CSFDs have also been demonstrated to vary across single, presumably uniform geologic units on Mars when count areas become small (Warner et al. 2015). Because both of these studies arguably include the effects of various local geological processes beyond the production of craters at a known rate, a study of theoretical lunar surfaces with different model ages was done and shows that both the accuracy and precision of the ages decrease with decreasing count area size and the percent errors increase for younger surfaces (Van der Bogert et al. 2015a, 2015b).

Limited count areas have implications for many young Copernican-era surfaces on the Moon. For example, only three of the 70 IMPs investigated by Braden et al. (2014) were large enough to provide useful CSFDs for fitting absolute model ages. The derived ages, 58–18 Ma, however are important for understanding possible late-stage volcanism on the Moon. An enigmatic region on the far side highlands containing ponded, smooth rocky deposits of uncertain origin has been suggested to be related to antipodal deposition of material from the Tycho impact (Bandfield et al. 2016; Robinson et al. 2016). Interpretation of a source for the material requires a robust determination of formation age; however, crater counts are confined to small areas where material ponded in topographic lows, and the variability of the derived ages, 10–42 Ma, may be an artifact of the small count areas. Nevertheless, the units are demonstrably young. Critically, the young craters Cone and North Ray, two of the locations used to define the CF, are relatively small and display a range of ages depending on the area of the ejecta blankets counts are conducted (Hiesinger et al. 2012, 2015). At Cone crater, the range of absolute model ages agrees well with the range of sample exposure ages, although the ages are slightly older in general. This may result in part from the lower accuracy and precision of the small count areas, unidentified secondary crater contamination, or a higher recent impact rate (Hiesinger et al. 2015).

On Mars, a multitude of relatively small landforms may be susceptible to similar errors. Many, associated with liquid water, are high priority targets for

exploration and understanding the planet's climate history such as deltas, alluvial fans, and fluvial channels (e.g., Grant and Wilson 2011; Mangold et al. 2012; Hauber et al. 2013; Grant et al. 2014; Ehlmann and Buz 2015). In many of these cases, the uncertainties caused by limited count areas cannot be mitigated by selecting larger areas. Nevertheless, such age estimates provide useful evidence for the youth of the studied areas.

Illumination and Image Resolution

Illumination conditions can have a significant influence on the ability to distinguish topographic features: higher incidence angles will increase shadowing and enhance variations in reflectance resulting from relief while decreasing variance in reflectance due to albedo features. The illumination geometry of an image therefore can influence the identification of craters and the resulting CSFDs derived from crater counts (Soderblom 1970; Young 1975; Wilcox et al. 2005; Ostrach et al. 2011; Antonenko et al. 2013; Robbins et al. 2014). A systematic study by Antonenko et al. (2013) demonstrated how incidence angles can influence a CSFD in a nontrivial way, and Ostrach et al. (2011) found smaller craters especially prone to illumination effects. Therefore, incidence angles can factor into derived model ages with higher angles (~60–80° depending on local conditions) being favorable. When comparing CSFDs from different areas, the illumination conditions of all images should be as similar as possible to avoid systematic differences (e.g., Hiesinger et al. 2012; Van der Bogert et al. 2017; Zanetti et al. 2017).

The superior resolution of the LROC and HiRISE cameras over previous orbital missions to the Moon and Mars, respectively, has provided the ability to observe crater populations down to meter-scale diameters, making studying very young surfaces feasible for dating. It should be noted that typically a roll-off, or downturn, in the CSFD away from the PF occurs at diameters approaching the image resolution limit as crater detections become increasingly incomplete. The smallest detectible craters therefore are not generally useful for age determinations. In the outer solar system, an absence of similarly high-resolution imaging makes studying extremely young terrains difficult. For example, there may indeed be small craters on Io or Enceladus' south pole or Sputnik Planum of Pluto, but the limited high-resolution coverage means we have not been able to determine their density much less their crater retention age. Furthermore, because imaging of the outer solar system satellites has been from fly-bys, the illumination angle is widely variable making this issue more of a problem than in the inner solar system.

CONCLUSIONS

The challenge in using crater populations to date young planetary surfaces largely results from the fact that crater counts are typically confined to smaller diameter craters, the behavior of which is less understood for the many reasons reviewed in this paper (Table 1). Many processes that influence crater populations preferentially alter smaller craters and therefore model ages derived from counting these craters require a cautious consideration of the geologic context of the feature or geologic unit being dated. Some of these factors (e.g., secondary cratering, resurfacing, and target strength-scaling) have the ability to affect geologic interpretations, while others most likely will not, given the inherent uncertainties of the crater chronometry technique: counting craters is imprecise by nature and standard deviations of CSFDs among individual observers counting craters are a few tens of percent depending on crater densities, diameters, and terrain type (e.g., Robbins et al. 2014). Though many of the issues listed in Table 1 are not new, and have been discussed in the literature since the initial development of the field of crater chronometry, the improved resolution and volume of image data over the last decade, especially from LROC at the Moon and HiRISE at Mars, have revived the discussion of many of these issues as they relate to small craters.

Ultimately, predicted ages depend on models of crater production and chronology. While some of the processes discussed can be accounted for in models, such as the atmospheric influence on crater production on Mars by Hartmann (2005), how other factors such as secondary cratering influence CSFDs and variations in impact rates result in uncertainty in CFs remains unclear or are currently debated. Ideally, the inspection of surrounding areas for possible primary craters that could have ejected material into a target area is part of a crater size-frequency measurement interpretation. Additional uncertainties in the modeled ages arise on young surfaces due to the limited count areas, small numbers of craters, and illumination and resolution limits, though often these can be mitigated by selecting appropriate images and count areas. The typically reported error bars correspond to Poisson statistics and do not capture the accumulated systematic uncertainty of the chronology model, which is difficult to quantify (Robbins et al. 2017b).

Perhaps the largest systemic cause of uncertainty is the large age gap in lunar samples between ~1 and 3 Ga coupled with uncertainty of Copernican ages relying on craters conducted exclusively on crater ejecta which may be biased by self-secondaries and target properties. Therefore, a significant advance in our understanding of the crater

Table 1. Summary of issues as outlined in paper.

Issue	Description	Comments
Impact rates		
Impactor populations	Knowledge of present-day impactor SFD incomplete	Survey of impactor populations at small sizes incomplete. Observations are consistent with a single power law over many orders of magnitude. Variations in power-law slope likely complicate the picture and there are discrepancies between models (Figure 1). Observed fresh lunar (Speyerer et al. 2016) and Martian (Daubar et al. 2013) CSFDs overlap with models but differ in slope.
Variations in impactor flux	Secular changes and punctuated variations in impact rates	Impact rate often assumed to be constant over last ~3 Gyr. Unclear if present-day flux is representative of last 3 Gyr: there is some evidence that variations may have occurred during this period, e.g., factor 2–3 higher impact rate in last ~300–400 Myr (Ghent et al. 2016; McEwen et al. 1997). Relative ages not affected, though adds uncertainty to chronology functions.
Atmospheric filtering		
Atmospheric passage	Drag, ablation, fragmentation of an atmosphere	Influence will differ between planetary bodies depending on atmospheric characteristics and becomes severe for impactor masses smaller than the mass of the atmospheric column. For Mars, Williams et al. (2014a, 2014b) find difference between highlands and lowlands varies model ages by up to ~30% depending on crater diameter.
Paleopressure variations	Paleopressures vary on Mars and influence of atmosphere not static	Martian pressure can vary significantly over time due to obliquity variations, though this history is largely uncertain. Atmospheric corrections may underestimate historic paleopressures, though significance unclear.
Crater formation heterogeneity		
Secondary cratering	Craters formed by ejected fragments from a distant primary crater	How many craters are distant background secondaries is unresolved. How secondaries influence model ages may be highly variable on young surfaces. Hartmann and Daubar (2017) suggest ages 0.1–1.0 Ma have highest uncertainties; for older surfaces, additional secondary crater events become small fraction of total. Outer solar system may be dominated by secondary craters (Bierhaus et al. 2005).
Self-secondary cratering	Craters formed from ejected fragments impacting the primary crater ejecta blanket	Zanetti et al. (2017) suggest lunar cratering rate for Copernican craters may be overestimated by factor of four. Influence of self-secondaries will diminish with time.
Target properties	Target strength influence on the resulting CSFD	Influence increases at smaller diameters. Appear to influence model ages up to a factor of a few at most (Williams et al. 2014a; Van der Bogert et al. 2017).
Crater modification	Postformation modification such as erosion, deposition, and terrain diffusion	Influence increases at smaller diameters. Highly variable. Age may not correspond to formation age, but rather other events/processes. Additional interpretation may be required.
Statistical and observational biases		
Limited number of craters	Young surfaces may be sparsely cratered	Shape of distribution of craters may not be determined; however, Poisson statistics can still provide time-resolved probability.
Limited count areas	Young surfaces may be limited to small areas	Accuracy shown to decrease with smaller crater-count area: Warner et al. (2015) recommend count areas exceed 1000 km^2; however, Van der Bogert et al. (2015b) find error only ~10% for areas as small as 1 km^2.
Illumination	Incidence angle of image influences crater detectability	Antonenko et al. (2013) find optimal incidence angles to be ~58° to ~77°.

chronology could be made with lunar samples returned from several locations bridging this time period. Furthermore, development of in situ dating such as discussed by Farley et al. (2014) and Anderson et al. (2015) for Mars and the Moon respectively, has the potential to calibrate model ages for other solar system bodies.

Given the knowledge that calibration to absolute time is complicated by numerous aspects, the crater statistics nevertheless have the potential to provide meaningful information and have successfully been applied in the past to establish the sequence of events on planetary surfaces. Crater densities vary over many orders of magnitude, and thus uncertainty of a factor of a few does not preclude the ability to distinguish very young terrains. For example, ice-rich dust mantling and glacial-like features at mid-to-high latitudes on Mars (e.g., Mustard et al. 2001; Head et al. 2003; Dickson et al. 2008; Souness et al. 2012) are predicted to result from the redistribution of water ice from the poles to lower latitudes during periods of high obliquities (Mischna et al. 2003; Laskar et al. 2004; Forget et al. 2006) resulting in surfaces < a few tens of Myr old. Crater populations have yielded consistent model ages for the predicted ice deposition (e.g., Hartmann et al. 2014).

While the technique of crater counting has proven to be an invaluable tool, widely applied by the planetary science community, its reliability varies considerably and has inherent limitations that need to be taken into account in applying derived ages to any geologic interpretation.

Acknowledgments—We would like to thank William K. Hartmann and Caleb I. Fassett for their insightful reviews and comments that improved the manuscript. J.-P. W. and A. P. were supported by a NASA Mars Data Analysis Program Grant No. NNX14AM12G. C. H. v. d. B. and H. H. were supported by German Aerospace Center (Deutsches Zentrum für Luft- und Raumfahrt) project 50OW1504, and G. M. by grant 50QM1301. Support for M. R. K. was provided by the NASA SSERVI program and a NASA Lunar Data Analysis Program Grant No NNX16AN52G.

Editorial Handling—Dr. Stuart Robbins

REFERENCES

Alvarellos J. L., Zahnle K. J., Dobrovolskis A. R., and Hamill P. 2005. Fates of satellite ejecta in the Saturn system. *Icarus* 178:104–123.

Alvarellos J. L., Dobrovolskis A., Zahnle K. J., Hamill P., Dones L., and Robbins S. 2017. Fates of satellite ejecta in the Saturn system, II. *Icarus*, 284:70–89.

Alvarez W. and Muller R. A. 1984. Evidence from crater ages for periodic impacts on Earth. *Nature* 308:718–720.

Anders E. 1964. Origin, age and composition of meteorites. *Space Science Reviews* 3:583–714.

Anderson F. S., Levine J., and Whitaker T. J. 2015. Rb-Sr resonance ionization geochronology of the Duluth Gabbro: A proof of concept for in situ dating of the Moon. *Rapid Communications in Mass Spectrometry* 29:1457–1464.

Antonenko I., Robbins S. J., Gay P. L., Lehan C., and Moore J. 2013. Effects of incidence angle on crater detection and the lunar isochron system: Preliminary results from the Cosmoquest Moonmappers citizen science project (abstract #2705). 44th Lunar and Planetary Science Conference. CD-ROM.

Artemieva N. 2013. Tycho crater ejecta (abstract #1413). 44th Lunar and Planetary Science Conference. CD-ROM.

Artemieva N. and Lunine J. I. 2005. Impact cratering on Titan II. Global melt, escaping ejecta, and aqueous alteration of surface organics. *Icarus* 175:522–533.

Artemieva N. A. and Shuvalov V. V. 2001. Motion of a fragmented meteoroid through the planetary atmosphere. *Journal of Geophysical Research Planets* 106:3297–3309.

Arvidson R., Crozaz G., Drozd R. J., Hohenberg C. M., and Morgan C. J. 1975. Cosmic ray exposure ages of features and events at the Apollo landing sites. *The Moon* 13:259–276.

Ashley J. W., Robinson M. S., Hawke B. R., van der Bogert C. H., Hiesinger H., Sato H., Speyerer E. J., Enns A. C., Wagner R. V., Young K. E., and Burns K. N. 2012. Geology of the King crater region—New insights into impact melt dynamics on the Moon. *Journal of Geophysical Research Planets* 117:E00H29.

Baldwin R. B. 1964. Lunar crater counts. *Astronomical Journal* 69:377–392.

Baldwin B. and Schaeffer Y. 1971. Ablation and breakup of large meteoroids during atmospheric entry. *Journal of Geophysical Research* 76:4653–4668.

Bandfield J. L., Ghent R. R., Vasavada A. R., Paige D. A., Lawrence S. J., and Robinson M. S. 2011. Lunar surface rock abundance and regolith fines temperatures derived from LRO Diviner Radiometer data. *Journal of Geophysical Research Planets*, 116:E00H02.

Bandfield J. L., Song E., Hayne P. O., Brand B. D., Ghent R. R., Vasavada A. R., and Paige D. A. 2014. Lunar cold spots: Granular flow features and extensive insulating materials surrounding young craters. *Icarus* 231:221–231.

Bandfield J. L., Cahill J. T. S., Carter L. M., Neish C. D., Patterson G. W., Williams J.-P., and Paige D. A. 2016. Distal ejecta from lunar impacts: Extensive regions of rocky deposits. *Icarus* 283:282–299. https://doi.org/10.1016/j.icarus.2016.05.013

Basilevsky A. T. 1976. On the evolution rate of small lunar craters. Proceedings, 7th Lunar Science Conference. pp. 1005–1020.

Basilevsky A. T. and Head J. W. 2012. Age of Giordano Bruno crater as deduced from the morphology of its secondaries at the Luna 24 landing site. *Planetary Space Science* 73:302–309.

Basilevsky A. T., Kreslavsky M. A., Karachevtseva I. P., and Gusakova E. N. 2014. Morphometry of small impact craters in the Lunokhod-1 and Lunokhod-2 study areas. *Planetary Space Science* 92:77–87.

Beech M. and Coulson I. M. 2010. The making of Martian meteorite Block Island. *Monthly Notices of the Royal Astronomical Society* 404:1457–1463.

Bierhaus E. B., Chapman C. R., Merline W. J., Brooks S. M., and Asphaug E. 2001. Pwyll secondaries and other small craters on Europa. *Icarus* 153:264–276.

Bierhaus E. B., Chapman C. R., and Merline W. J. 2005. Secondary craters on Europa and implications for cratered surfaces. *Nature* 437:1125–1127.

Bierhaus E. B., Dones L., Alvarellos J. L., and Zahnle K. 2012. The role of ejecta in the small crater populations on the mid-sized saturnian satellites. *Icarus* 218:602–621.

Bierhaus E. B., McEwen A. S., Robbins S. J., Singer K. N., Dones L., Kirchoff M. R., and Williams J.-P. 2017. Secondary craters and ejecta across the solar system: Populations and effects on impact-crater based chronologies. *Meteoritics & Planetary Science*. Forthcoming.

Bloom C., Golombek M., Warner N., and Wigton N. 2014. Size frequency distribution and ejection velocity of Corinto crater secondaries in Elysium Planitia (abstract #1289). Eighth International Conference on Mars.

Bogard D. D. 1995. Impact ages of meteorites: A synthesis. *Meteoritics* 30:244–268.

Boschi S., Schmitz B., Heck P. R., Cronholm A., Defouilloy C., Kita N. T., Monechi S., Montanari A., Rout S. S., and Terfelt F. 2017. Late Eocene ^{3}He and Ir anomalies associated with ordinary chondritic spinels. *Geochimica et Cosmochimica Acta* 204:205–218.

Bottke W. F., Rubincam D. P., and Burns J. A. 2000. Dynamical evolution of main belt meteoroids: Numerical simulations incorporating planetary perturbations and Yarkovsky thermal forces. *Icarus* 145:301–331.

Bottke W. F., Vokrouhlický D., Rubincam D., and Brož M. 2002. Dynamical evolution of asteroids and meteoroids using the Yarkovsky effect. In *Asteroids III*, edited by Binzel R., Hehrels T., and Matthews M. S. Tucson, Arizona: The University of Arizona Press. pp. 395–408.

Bottke W. F., Durda D. D., Nesvorný D., Jedicke R., Morbidelli A., Vokrouhlický D., and Levison H. 2005a. The fossilized size distribution of the main asteroid belt. *Icarus* 175:111–140.

Bottke W. F., Durda D. D., Nesvorný D., Jedicke R., Morbidelli A., Vokrouhlický D., and Levison H. F. 2005b. Linking the collisional history of the main asteroid belt to its dynamical excitation and depletion. *Icarus* 179:63–94.

Bottke W. F., Vokrouhlický D., Rubincam D. P., and Nesvorný D. 2006. The Yarkovsky and YORP Effects: Implications for asteroid dynamics. *Annual Review of Earth and Planetary Science* 34:157–191.

Bottke W. F., Vokrouhlický D., and Nesvorný D. 2007. An asteroid breakup 160 Myr ago as the probable source of the K/T Impactor. *Nature* 449:48–53.

Bottke W. F., Brož M., O'Brien D. P., Campo Bagatin A., Morbidelli A., and Marchi S. 2015. The collisional evolution of the main asteroid belt. In *Asteroids IV*, edited by Michel P., DeMeo F. E. and Bottke W. F. Tucson, Arizona: The University of Arizona Press. pp. 701–724.

Bottomley R., Grieve R. A. F., York D., and Masaitis V. 1997. The age of Popigai impact event and its relation to events at Eocene-Oligocene boundary. *Nature* 338:365–368.

Bowell E., Hapke B., Domingue D., Lumme K., Peltoniemi J., Harris A. W. 1989. Application of photometric models to asteroids. In *Asteroids II*, edited by Binzel R., Hehrels T., and Matthews M. S. Tucson, Arizona: The University of Arizona Press. pp. 524–556.

Boyce J. M. and Mouginis-Mark P. J. 2015. Anomolous areas of high crater density on the rim of the Martian impact crater tooting (abstract #9005). Workshop on Issues in Crater Studies and the Dating of Planetary Surfaces.

Braden S. E., Stopar J. D., Robinson M. S., Lawrence S. J., van der Bogert C. H., and Hiesinger H. 2014. Evidence for basaltic volcanism on the Moon within the past 100 million years. *Nature Geoscience* 7:787–791.

Brinkmann R. T. 1966. Lunar crater distributions from Ranger 7 photographs. *Journal of Geophysical Research* 71:340–342.

Bronshten V. A. 1983. *Physics of meteoric phenomena*. Dordrecht: Reidel Publishing Company.

Brown P., Spalding R. E., ReVelle D. O., Tagliaferri E., and Worden S. P. 2002. The flux of small near-Earth objects colliding with the Earth. *Nature* 420:294–296.

Brown P. G., Assink J. D., Astiz L., Blaauw R., Boslough M. B., Borovička J., Brachet N., Brown D., Campbell-Brown M., Ceranna L., Cooke W., de Groot-Hedlin C., Drob D. P., Edwards W., Evers L. G., Garces M., Gill J., Hedlin M., Kingery A., Laske G., Le Pichon A., Mialle P., Moser D. E., Saffer A., Silber E., Smets P., Spalding R. E., Spurný P., Tagliaferri E., Uren D., Weryk R. J., Whitaker R., and Krzeminski Z. 2013. A 500-kiloton airburst over Chelyabinsk and an enhanced hazard from small impactors. *Nature* 503:238–241.

Campbell B. A. 1999. Surface formation rates and impact crater densities on Venus. *Journal of Geophysical Research Planets* 104:21,951–21,955.

Ceplecha Z., Borovička J., Elford W. G., Revelle D. O., Hawkes R. L., Porubčan V., and Šimek M. 1998. Meteor phenomena and bodies. *Space Science Reviews* 84:327–471.

Chapman C. R. and Jones K. L. 1977. Cratering and obliteration history of Mars. *Annual Reviews of Earth and Planetary Science* 5:515–540.

Chapman C. R., Pollack J. B., and Sagan C. 1969. An analysis of the Mariner-4 cratering statistics. *The Astronomical Journal* 74:1039–1051.

Chapman C. R., Mosher J. A., and Simmons G. 1970. Lunar cratering and erosion from Orbiter 5 photographs. *Journal of Geophysical Research Planets* 75:1445–1466.

Chapman C. R., Veverka J., Belton M. J. S., Neukum G., and Morrison D. 1996. Cratering on Gaspra. *Icarus* 120:231–245.

Chappelow J. E. and Golombek M. P. 2010. Event and conditions that produced the iron meteorite Block Island on Mars. *Journal of Geophysical Research Planets*, 115: E00F07.

Chappelow J. E. and Sharpton V. L. 2005. Influences of atmospheric variations on Mars's record of small craters. *Icarus* 178:40–55.

Chappelow J. E. and Sharpton V. L. 2006. The event that produced heat shield rock and its implications for the Martian atmosphere. *Geophysical Research Letters* 33:L19201.

Christensen P. R., Jakosky B. M., Kieffer H. H., Malin M. C., McSween H. Y. Jr., Nealson K., Mehall G. L., Silverman S. H., Ferry S., Caplinger M., and Ravine M. 2004. The Thermal Emission Imaging System (THEMIS) for the 2001 Mars Odyssey Mission. *Space Science Reviews* 110:85–130.

Chyba C. F., Thomas P. J., and Zahnle K. J. 1993. The 1908 Tunguska explosion—Atmospheric disruption of a stony asteroid. *Nature* 361:40–44.

Cintala M. J., Head J. W., and Veverka J. 1978. Characteristics of the cratering process on small satellites and asteroids. Proceedings, 9th Lunar and Planetary Science Conference. pp. 3803–3830.

Cocks F. H. 2010. ^{3}He in permanently shadowed lunar polar surfaces. *Icarus* 206:778–779.

Crater Analysis Techniques Working Group. 1979. Standard techniques for presentation and analysis of crater size-frequency data. *Icarus* 37:467–474.

Culler T. S., Becker T. A., Muller R. A., and Renne P. R. 2000. Lunar impact history from ^{40}Ar/^{39}Ar dating of glass spherules. *Science* 287:1785–1788.

D'Abramo G., Harris A. W., Boattini A., Werner S. C., Harris A. W., and Valsecchi G. B. 2001. A simplistic probabilistic model to estimate the population of near-Earth asteroids. *Icarus* 153:214–217.

Daubar I. J., McEwen A. S., Byrne S., Dundas C. M., Keske A. L., Amaya G. L., Kennedy M., and Robinson M. S. 2011. New craters on Mars and the Moon (abstract #2232). 42nd Lunar and Planetary Science Conference. CD-ROM.

Daubar I. J., McEwen A. S., Byrne S., Kennedy M. R., and Ivanov B. 2013. The current Martian cratering rate. *Icarus* 225:506–516.

Daubar I. J., Atwood-Stone C., Byrne S., McEwen A. S., and Russell P. S. 2014. The morphology of small fresh craters on Mars and the Moon. *Journal of Geophysical Research Planets* 119:2620–2639.

Daubar I. J., Dundas C. M., Byrne S., Geissler P., Bart G. D., McEwen A. S., Russell P. S., Chojnacki M., and Golombek M. P. 2016. Changes in blast zone albedo patters around new Martian impact craters. *Icarus* 267:86–105.

Davis P. M. 1993. Meteoroid impacts as seismic sources on Mars. *Icarus* 105:469–478.

Dickson J. L., Head J. W., and Marchant D. R. 2008. Late Amazonian glaciation at the dichotomy boundary on Mars: Evidence for glacial thickness maxima and multiple glacial phases. *Geology* 36:411–414.

Dobrovolskis A. R. and Lissauer J. J. 2004. The fate of ejecta from Hyperion. *Icarus* 169:462–473.

Dones L., Chapman C. R., McKinnon W. B., Melosh H. J., Kirchoff M R., Neukum G., and Zahnle K. J. 2009. Icy satellites of Saturn: Impact cratering and age determination. In *Saturn from Cassini-Huygens*, edited by Daugherty M. K., Esposito L. W., and Krimigis S. M. Heidelberg, Germany: Springer. pp. 613–36.

Dundas C. M., Keszthelyi L. P., Bray V. J., and McEwen A. S. 2010. Role of material properties in the cratering record of young platy-ridged lava on Mars. *Geophysical Research Letters* 37:L12203.

Durda D. D., Greenberg R., and Jedicke R. 1998. Collisional models and scaling laws: A new interpretation of the shape of the main-belt asteroid size distribution. *Icarus* 135:431–440.

Ehlmann B. L. and Buz J. 2015. Mineralogy and fluvial history of the watersheds of Gale, Knobel, and Sharp craters: A regional context for the Mars Science Laboratory Curiosity's exploration. *Geophysical Research Letters* 42:264–273.

Fanale F. P. and Salvail J. R. 1994. Quasi-periodic atmosphere-regolith-cap CO_2 redistribution in the Martian past. *Icarus* 111:305–316.

Farley K. A. 2009. Late Eocene and late Miocene cosmic dust events: Comet showers, asteroid collisions, or lunar impacts? *Geological Society of America Special Paper* 452:27–35.

Farley K. A., Montanari A., Shoemaker E. M., and Shoemaker C. S. 1998. Geochemical evidence for a comet shower in the late Eocene. *Science* 208:1250–1253.

Farley K. A., Malespin C., Mahaffy P., Grotzinger J. P., Vasconcelos P. M., Milliken R. E., Malin M., Edgett K. S., Pavlov A. A., Hurowitz J. A., Grant J. A., Miller H. B., Arvidson R., Beegle L., Calef F., Conrad P. G., Dietrich W. E., Eigenbrode J., Gellert R., Gupta S., Hamilton V., Hassler D. M., Lewis K. W., McLennan S. M., Ming D., Navarro-Gonz_alez R., Schwenzer S. P., Steele A., Stolper E. M., Sumner D. Y., Vaniman D., Vasavada A., Williford K., Wimmer-Schweingruber R. F., and The MSL Science Team. 2014. In situ radiometric and exposure age dating of the Martian surface. *Science* 343:1247166-1–1247166-5. https://doi.org/10.1126/science.1247166.

Fassett C. I. 2016. Analysis of impact crater populations and the geochronology of planetary surfaces in the inner solar system. *Journal of Geophysical Research Planets* 121:1–27. https://doi.org/10.1002/2016JE005094.

Fassett C. I. and Thomson B. J. 2014. Crater degradation on the lunar maria: Topographic diffusion and the rate of erosion on the Moon. *Journal of Geophysical Research Planets* 119:1–17. https://doi.org/10.1002/2014JE004698.

Fassett C. I., Kadish S. J., Head J. W., Solomon S. C., and Strom R. G. 2011. The global population of large craters on Mercury and comparison with the Moon. *Geophysical Research Letters* 38:L10202.

Fielder G. 1962. Ray elements and secondary-impact craters on the Moon. *The Astrophysical Journal* 135:632–637.

Forget F., Haberle R. M., Montmessin F., Levrard B., and Head J. W. 2006. Formation of glaciers on mars by atmospheric precipitation at high obliquity. *Science* 311:368–371.

Forsberg-Taylor N. K., Howard A. D., and Craddock R. C. 2004. Crater degradation in the Martian highlands: Morphometric analysis of the Sinus Sabaeus region and simulation modeling suggest fluvial processes. *Journal of Geophysical Research Planets* 119:2522–2547.

François L. M., Walker J. C. G., and Kuhn W. R. 1990. A numerical simulation of climate changes during the obliquity cycle on Mars. *Journal of Geophysical Research Solid Earth* 95:14,761–14,778.

Fritz J., Tagle R., and Artemieva N. 2007. Lunar helium-3 in marine sediments: Implications for a late Eocene asteroid shower. *Icarus* 189:591–594.

Fulchignoni M., Ferri F., Angrilli F., Ball A. J., Bar-Nun A., Barucci M. A., Bettanini C., Bianchini G., Borucki W., Colombatti G., Coradini M., Coustenis A., Debei S., Falkner P., Fanti G., Flamini E., Gaborit V., Grard R., Hamelin M., Harri A. M., Hathi B., Jernej I., Leese M. R., Lehto A., Lion Stoppato P. F., López-Moreno J. J., Mäkinen T., McDonnell J. A. M., McKay C. P., Molina-Cuberos G., Neubauer F. M., Pirronello V., Rodrigo R., Saggin B., Schwingenschuh K., Seiff A., Simões F., Svedhem H., Tokano T., Towner M. C., Trautner R., Withers P., and Zarnecki J. C. 2005. In situ measurements of the physical characteristics of Titan's environment. *Nature* 438:785–791.

Ghent R. R., Hayne P. O., Bandfield J. L., Campbell B. A., Allen C. C., Carter L. M., and Paige D. A. 2014. Constraints on the recent rate of lunar ejecta breakdown and implications for crater ages. *Geology* 42:1059–1062.

Ghent R. R., Mazrouei S., Bandfield J. L., Carter L. M., Williams J.-P., and Paige D. A. 2016. Remote sensing constraints on lunar chronology (abstract #6040). New Views of the Moon 2.

Golombek M. P., Grant J. A., Crumpler L. S., Greeley R., Arvidson R. E., Bell J. F., and Squyres S. W. 2006. Erosion rates at the Mars Exploration Rover landing sites and long-term climate change on Mars. *Journal of Geophysical Research Planets*, 111:E12S10.

Golombek M., Bloom C., Wigton N., and Warner N. 2014a. Constraints on the age of Corinto crater from mapping

secondaries in Elysium Planitia on Mars (abstract #1470). Eighth International Conference on Mars.
Golombek M. P., Warner N. H., Ganti V., Lamb M. P., Parker T. J., Fergason R. L., and Sullivan R. 2014b. Small crater modification on Meridiani Planum and implications for erosion rates and climate change on Mars. *Journal of Geophysical Research Planets* 109:E05002.
Grant J. A. and Wilson S. A. 2011. Late alluvial fan formation in Margaritifer Terra. *Mars*. *Geophysical Research Letters* 38:L08201.
Grant J. A., Wilson S. A., Mangold N., Calef F. III, and Grotzinger J. P. 2014. The timing of alluvial activity in Gale crater Mars. *Geophysical Research Letters* 41:1142–1148.
Greeley R. and Gault D. E. 1970. Precision size-frequency distributions of craters for 12 selected areas of the lunar surface. *Moon* 2:10–77.
Guinness E. A. and Arvidson R. E. 1977. On the consistency of the lunar cratering flux over the past 3.3×10^9 yr. Proceedings, 8th Lunar Science Conference. pp. 3475–3494.
Haack H., Farinella P., Scott E. R. D., and Keil K. 1996. Meteoritic, asteroidal and theoretical constraints on the 500 Ma disruption of the L chondrite parent body. *Icarus* 119:182–191.
Haberle R. M., Tyler D., McKay C. P., and Davis W. L. 1994. A model for the evolution of CO_2 on Mars. *Icarus* 109:102–120.
Haberle R. M., Kahre M. A., Hollingsworth J. L., Schaeffer J., Montmessin F., and Phillips R. J. 2012. A cloud greenhouse effect on Mars: Significant climate change in the recent past? (abstract #1665). 43rd Lunar and Planetary Science Conference. CD-ROM.
Halliday I., Griffin A. A., and Blackwell A. T. 1996. Detailed data for 259 fireballs from the Canadian camera network and inferences concerning the influx of large meteoroids. *Meteoritics & Planetary Science* 31:185–217.
Hamilton C., Scheidt S. P., Bleacher J. E., IrwinIII R. P., and Garry W. B. 2015. "Fill and spill" lava emplacement associated with the December 1974 flow on Kilauea volcano, Hawai'i, USA (abstract #1072). 46th Lunar and Planetary Science Conference. CD-ROM.
Harris A. W. and D'Abramo G. 2015. The population of near-Earth asteroids. *Icarus* 257:302–312.
Harris A. W., Boslough M., Chapman C. R., Drube L., Michel P., and Harris A. W. 2015. Asteroid impacts and modern civilization: Can we prevent a catastrophe? In *Asteroids IV*, edited by Michel P., DeMeo F. E., and Bottke W. F. Tucson, Arizona: The University of Arizona Press. pp. 835–854.
Hartmann W. K. 1965. Terrestrial and lunar flux of large meteorites in the last two billion years. *Icarus* 4:157–165.
Hartmann W. K. 1966a. Martian cratering. *Icarus* 5:565–576.
Hartmann W. K. 1966b. Early lunar cratering. *Icarus* 5:406–418.
Hartmann W. K. 1968. Lunar crater counts. VI: The young craters Tycho, Aristarchus, and Copernicus. *Communication of Lunar and Planetary Laboratory* 8:145–156.
Hartmann W. K. 1970. Preliminary note on lunar cratering rates and absolute time-scales. *Icarus* 12:131–133.
Hartmann W. K. 1971. Martian cratering III: Theory of crater obliteration. *Icarus* 15:410–428.
Hartmann W. K. 1984. Does crater "saturation equilibrium" occur in the solar system. *Icarus* 60:56–74.
Hartmann W. K. 1999. Martian cratering VI: Crater count isochrons and evidence for recent volcanism from Mars Global Surveyor. *Meteoritics & Planetary Science* 34:167–177.
Hartmann W. K. 2005. Martian cratering 8: Isochron refinement and the chronology of Mars. *Icarus* 174:294–320.
Hartmann W. K. 2007. Martian cratering 9. Toward resolution of the controversy about small craters. *Icarus* 189:274–278.
Hartmann W. K. and Daubar I. J. 2017. Martian cratering 11. Utilizing decameter scale craterpopulations to study Martian history. *Meteoritics & Planetary Science* 52:493–510.
Hartmann W. K. and Neukum G. 2001. Cratering chronology and the evolution of Mars. *Space Science Reviews* 96:165–194.
Hartmann W. K., Strom R., Weidenschilling S. J., Blasius K., Woronow A., Dence M., Grieve R., Diaz J., Chapman C. R., Shoemaker E., and Jones K. 1981. Chronology of planetary volcanism by comparative studies of planetary crater. In *Basaltic volcanism on the terrestrial planets*. New York: Pergamon Press Inc. pp. 1050–1127.
Hartmann W. K., Quantin C., and Mangold N. 2007. Possible long-term decline in impact rates 2. Lunar impact-melt data regarding impact history. *Icarus* 186:11–23.
Hartmann W. K., Neukum G., and Werner S. C. 2008. Confirmation and utilization of the "production function" size-frequency distributions of Martian impact craters. *Geophysical Research Letters* 35:L02205.
Hartmann W. K., Quantin C., Werner S. C., and Popova O. 2010. Do young Martian ray craters have ages consistent with the crater count system? *Icarus* 208:621–635.
Hartmann W. K., Ansan V., Mangold N., Forget F., and Berman D. C. 2014. Comprehensive analysis of glaciated Martian crater Greg. *Icarus* 228:96–120.
Hartmann W. K., Daubar I. J., Popova O., and Joseph J. M. 2017. Martian cratering 12. Utilizing primary crater clusters to study crater populations and meteoroid properties. *Meteoritics & Planetary Science*. Forthcoming
Hartman W. K. and Hartmann A. C. 1968. Asteroid collisions and evolution of asteroidal mass distribution and meteoritic flux. *Icarus* 8:361–381.
Hauber E., Platz T., Reiss D., Le Deit L., Kleinhans M. G., Marra W. A., de Haas T., and Carbonneau P. 2013. Asynchronous formation of Hesperian and Amazonian-aged deltas on Mars and implications for climate. *Journal of Geophysical Research Planets* 118:1529–1544.
Head J. W., Mustard J. F., Kreslavsky M. A., Milliken R. E., and Marchant D. R. 2003. Recent ice ages on Mars. *Nature* 426:797–802.
Heck P. R., Schmitz B., Bauer H., Halliday A. N., and Wieler R. 2004. Fast delivery of meteorites to Earth after a major asteroid collision. *Nature* 430:323–325.
Heiken G., Vaniman D., and French B. M. 1991. *The lunar sourcebook*. *A user's guide to the Moon*. New York: LPI and Cambridge University Press. 736 p.
Herkenhoff K. E. and Plaut J. J. 2000. Surface ages and resurfacing rates of the Polar Layered Deposits on Mars. *Icarus* 144:243–253.
Herrick R. R., Sharpton V. L., Malin M. C., Lyons S. N., and Feely K. 1997. Morphology and morphometry of impact craters. In *Venus II*, edited by Bougher S. W., Hunten D. M., and Phillips R. J. Tucson, Arizona: The University of Arizona Press. pp. 1015–1046.

Hiesinger H., Head J. W. III, Wolf U., Jaumann R., and Neukum G. 2002. Lunar mare basalt flow units: Thicknesses determined from crater size-frequency distributions. *Geophysical Research Letters* 29:1248.

Hiesinger H., van der Bogert C. H., Pasckert J. H., Funcke L., Giacomini L., Ostrach L. R., and Robinson M. S. 2012. How old are young lunar craters? *Journal of Geophysical Research Planets*, 117:E00H10.

Hiesinger H., Simon I., van der Bogert C. H., Robinson M. S., and Plescia J. B. 2015. New crater size-frequency distribution measurements for Cone crater at the Apollo 14 landing site (abstract #1834). 46th Lunar and Planetary Science Conference. CD-ROM.

Hiesinger H., Marchi S., Schmedemann N., Schenk P., Pasckert J. H., Neesemann A., O'Brien D. P., Kneissl T., Ermakov A. I., Fu R. R., Bland M. T., Nathues A., Platz T., Williams D. A., Jaumann R., Castillo-Rogez J. C., Ruesch O., Schmidt B., Park R. S., Preusker F., Buczkowski D. L., Russell C. T., and Raymond C. A. 2016a. Cratering on Ceres: Implications for its crust and evolution. *Science* 353:aaf4759-1–aaf4759-8. https://doi.org/10.1126/science.aaf4759.

Hiesinger H., Pasckert J. H., van der Bogert C. H., and Robinson M. S. 2016b. New crater size-frequency distribution measurements for Autolycus crater, Moon (abstract #1879). 47th Lunar and Planetary Science Conference. CD-ROM.

Holsapple K. A. 1993. The scaling of impact processes in planetary science. *Annual Reviews Earth and Planetary Sciences* 21:333–373.

Holsapple K. A. and Schmidt R. M. 1982. On the scaling of crater dimensions 2. Impact processes. *Journal of Geophysical Research Solid Earth* 87:1849–1870.

Hörz F., Cintala M. J., Rochelle W. C., and Kirk B. 1999. Collisionally processed rocks on Mars. *Science* 285:2105–2107.

Housen K. R. and Holsapple K. A. 2011. Ejecta from impact craters. *Icarus* 211:856–875.

Howard A. D. 2004. Simple non-fluvial models of planetary science modification, with application to Mars (abstract #1054). 35th Lunar and Planetary Science Conference. CD-ROM.

Howard A. D. and Craddock R. A. 1998. Simulation of erosion of ancient cratered terrain on Mars (abstract #1323). 29th Lunar and Planetary Science Conference. CD-ROM.

Ip W.-H. 1990. Meteoroid ablation processes in Titan's atmosphere. *Science* 345:511–512.

Ivanov B. A. 2001. Mars/Moon cratering rate ratio estimates. *Space Science Reviews* 96:87–104.

Ivanov B. A. 2006. Earth/Moon impact rate comparison: Searching constraints for lunar secondary/primary cratering proportion. *Icarus* 183:504–507.

Ivanov B. A. 2008. Size-frequency distribution of asteroids and impact craters: Estimates of impact rate. In *Catastrophic events caused by cosmic objects*, edited by Adushkin V. V. and Nemchinov I. V. Dordrecht: Springer. pp. 91–116.

Ivanov B. A. and Hartmann W. K. 2007. Exogenic dynamics, cratering and surface ages. *In Treatise on Geophysics* 10:207–242.

Ivanov M. A. and Head J. W. 2011. Global geologic map of Venus. *Planetary and Space Sciences* 59:1559–1600.

Ivanov B. A. and Melosh H. J. 2003. Impacts do not initiate volcanic eruptions: Eruptions close to the crater. *Geology* 31:869–872.

Ivanov B. A., Melosh H. J., McEwen A. S., and the HiRISE team. 2014. New small impact craters in high resolution HiRISE images—IV (abstract #1812). 45th Lunar and Planetary Science Conference. CD-ROM.

JeongAhn Y. and Malhotra R. 2015. The current impact flux on Mars and its seasonal variation. *Icarus* 262:140–153.

Jögi P. M. and Paige D. A. 2015. Directed cratering ejecta ballistic model for antipodal impact, frictionally heated, melt deposits on the Moon (abstract #2779). 46th Lunar and Planetary Science Conference. CD-ROM.

Keil K., Haack H., and Scott E. R. D. 1994. Catastrophic fragmentation of asteroids: Evidence from meteorites. *Planetary Space Science* 42:1109–1122.

Keszthelyi L., Thordarson T., McEwen A., Haack H., Guilbaud M.-N., Self S., and Rossi M. J. 2004. Icelandic analogs to Martian flood lavas. *Geochemistry, Geophysics, Geosystems* 5:Q11014.

Kieffer H. H. and Zent A. P. 1992. Quasi-periodic climate change on Mars. In *Mars*, edited by Matthews M. S., Kieffer H. H., Jakosky B. M., and Snyder C.. Tucson, Arizona: The University of Arizona Press. pp. 1180–1218.

Kirchoff M. R. and Schenk P. 2010. Impact cratering records of the mid-sized, icy saturnian satellites. *Icarus* 206:485–497.

Kirchoff M. R., Chapman C. R., Marchi S., Curtis K. M., Enke B., and Bottke W. F. 2013. Ages of large lunar impact craters and implications for bombardment during the Moon's middle age. *Icarus* 225:325–341.

Kirchoff M. R., Marchi S., and Wünnemann K. 2015. The effects of terrain properties on determining crater model ages of lunar surfaces (abstract #2121). 46th Lunar and Planetary Science Conference. CD-ROM.

Kite E. S. and Mayer D. P. 2017. Mars sedimentary rock erosion rates constrained using crater counts, with applications to organic-matter preservation and to the global dust cycle. *Icarus* 286:212–222.

Kneissl T., Michael G. G., and Schedemann N. 2016. Treatment of non-sparse cratering in planetary surface dating. *Icarus* 277:187–195.

Koeberl C. 2009. Late Eocene impact craters and impactoclastic layers—An overview. *Geological Society of America Special Paper* 452:17–26.

Koeberl C., Poag C. W., Reimold W. U., and Brandt D. 1996. Impact origin of the Chesapeake Bay structure and the source of the North American tektites. *Science* 271:1263–1266.

Korteniemi J. and Kreslavsky M. A. 2013. Patterned ground in Martian high northern latitudes: Morphology and age constraints. *Icarus* 225:960–970.

Kreslavsky M. A. and Head J. W. 2005. Mars at very low obliquity: Atmospheric collapse and the fate of volatiles. *Geophysical Research Letters* 32:L12202.

Kuiper G. P. 1965. Interpretation of Ranger VII records. In *Ranger VII, Part II—Experimenters' analyses and interpretations*. Jet Propulsion Laboratory California Institute of Technology, Technical Report, 32-700.

Kyte F. T., Shukolyukov A., Hildebrand A. R., Lugmair G. W., and Hanova J. 2011. Chromium-isotopes in Late Eocene impact spherules indicate a likely asteroid belt provenance. *Earth and Planetary Science Letters* 302:279–286.

Landis M. E., Byrne S., Daubar I. J., Herkenhoff K. E., and Dundas C. M. 2016. A revised surface age for the north polar layered deposits of Mars. *Geophysical Research Letters* 43:3060–3068. https://doi.org/10.1002/2016GL068434.

Laskar J., Correia A. C. M., Gastineau M., Joutel F., Levrard B., and Robutel P. 2004. Long term evolution and chaotic diffusion of the insolation quantities of Mars. *Icarus* 170:343–364.

Le Feuvre M. and Wieczorek M. A. 2011. Nonuniform cratering of the Moon and a revised crater chronology of the inner solar system. *Icarus* 214:1–20.

Leighton R. B. and Murray B. C. 1966. Behavior of carbon dioxide and other volatiles on Mars. *Science* 153:136–144.

Levine J., Becker T. A., Muller R. A., and Renne P. R. 2005. $^{40}Ar/^{39}Ar$ dating of Apollo 12 impact spherules. *Geophysical Research Letters* 32:L15201.

Levrard B., Forget F., Montmessin F., and Laskar J. 2004. Recent ice-rich deposits formed at high latitudes on Mars by sublimation of unstable equatorial ice during low obliquity. *Nature* 431:1072–1075.

Lissauer J. J., Squyres S. W., and Hartmann W. K. 1988. Bombardment history of the Saturn system. *Journal of Geophysical Research Solid Earth* 93:13,776–13,804.

Lucchitta B. K. and Sanchez A. G. 1975. Crater studies in the Apollo 17 region. Proceedings, 6th Lunar Science Conference. pp. 2427–2441.

Mahanti P., Robinson M. S., Thompson T. J., and van der Bogert C. H. 2016. What accelerates the degradation of small lunar craters? Unexpected, contrasting rates observed at Apollo 16 and 17 regions (abstract #1202). 47th Lunar and Planetary Science Conference. CD-ROM.

Malin M. C., Danielson G. E., Ingersoll A. P., Masursky H., Veverka J., Ravine M. A., and Soulanille T. A. 1992. Mars orbiter camera. *Journal of Geophysical Research Planets* 97:7699–7718.

Malin M. C., Edgett K. S., Posiolova L. V., McColley S. M., and Dobrea E. Z. N. 2006. Present-day impact cratering rate and contemporary gully activity on Mars. *Science* 314:1573–1577.

Malin M. C., Bell J. F. III, Cantor B. A., Caplinger M. A., Calvin W. M., Clancy R. T., Edgett K. S., Edwards L., Haberle R. M., James P. B., Lee S. W., Ravine M. A., Thomas P. C., and Wolff M. J. 2007. Context camera investigation on board the Mars Reconnaissance Orbiter. *Journal of Geophysical Research Planets* 112:E05S04.

Mangold N., Kite E. S., Kleinhans M. G., Newsom H., Ansan V., Hauber E., Kraal E., Quantin C., and Tanaka K. 2012. The origin and timing of fluvial activity at Eberswalde crater, Mars. *Icarus* 220:530–551.

Marchi S., Mottola S., Cremonese G., Massironi M., and Martellato E. 2009. A new chronology for the Moon and Mercury. *The Astronomical Journal* 137:4936–4948.

Marchi S., Massironi M., Cremonese G., Martellato E., Giacomini L., and Prockter L. 2011. The effects of the target material properties and layering on the crater chronology: The case of Raditladi and Rachmaninoff basins on Mercury. *Planetary and Space Science* 59:1968–1980.

Marchi S., Bottke W. F., O'Brien D. P., Schenk P., Mottola S., DeSanctis M. C., Kring D. A., Williams D. A., Raymond C. A., and Russell C. T. 2014. Small crater populations on Vesta. *Planetary and Space Sciences* 103:96–103.

Matese J. J., Whitman P. G., Innanen K. A., and Valtonen M. J. 1995. Periodic modulation of the Oort cloud comet flux by the adiabatically changing Galactic tide. *Icarus* 116:255–268.

Mazrouei S., Ghent R. R., and Bottke W. F. 2015. Has the lunar impact flux rate changed in the past billion years? (abstract #2331). 46th Lunar and Planetary Science Conference. CD-ROM.

McEwen A. S. and Bierhaus E. B. 2006. The importance of secondary cratering to age constraints on planetary surfaces. *Annual Reviews of Earth and Planetary Sciences* 34:535–567.

McEwen A. S., Moore J. M., and Shoemaker E. M. 1997. The Phanerozoic impact cratering rate: Evidence from the farside of the Moon. *Journal of Geophysical Research Planets* 102:9231–9242.

McEwen A. S., Preblich B. S., Turtle E. P., Artemieva N. A., Golombek M. P., Hurst M., Kirk R. L., Burr D. M., and Christensen P. R. 2005. The rayed crater Zunil and interpretations of small impact craters on Mars. *Icarus* 176:351–381.

McEwen A. S., Eliason E. M., Bergstrom J. W., Bridges N. T., Hansen C. J., Delamere W. A., Grant J. A., Gulick V. C., Herkenhoff K. E., Keszthelyi L., Kirk R. L., Mellon M. T., Squyres S. W., Thomas N., and Weitz C. M. 2007. Mars reconnaissance orbiter's high resolution imaging science experiment (HiRISE). *Journal of Geophysical Research Planets* 112:E05S02.

McEwen A. S., Banks M. E., Baugh N., Becker K., Boyd A., Bergstrom J. W., Beyer R. A., Bortolini E., Bridges N. T., Byrne S., Castalia B., Chuang F. C., Crumpler L. S., Daubar I., Davatzes A. K., Deardorff D. G., DeJong A., Delamere W. A., Noe Dobrea E., Dundas C. M., Eliason E. M., Espinoza Y., Fennema A., Fishbaugh K. E., Forrester T., Geissler P. E., Grant J. A., Griffes J. L., Grotzinger J. P., Gulick V. C., Hansen C. J., Herkenhoff K. E., Heyd R., Jaeger W. L., Jones D., Kanefsky B., Keszthelyi L., King R., Kirk R. L., Kolb K. J., Lasco J., Lefort A., Leis R., Lewis K. W., Martinez-Alonso S., Mattson S., McArthur G., Mellon M. T., Metz J. M., Milazzo M. P., Milliken R. E., Motazedian T., Okubo C. H., Ortiz A., Philippoff A. J., Plassmann J., Polit A., Russell P. S., Schaller C., Searls M. L., Spriggs T., Squyres S. W., Tarr S., Thomas N., Thomson B. J., Tornabene L. L., Van Houten C., Verba C., Weitz C. M., and Wray J. J. 2010. The high resolution imaging science experiment (HiRISE) during MRO's primary science phase (PSP). *Icarus* 205:2–37.

McEwen A., Daubar I., Ivanov B., Oberst J., Malhotra R., JeongAhn Y., and Byrne S. 2015. Current impact rate on Earth, Moon, and Mars (abstract #1854). 46th Lunar and Planetary Science Conference. CD-ROM.

Melosh H. J. 1989. *Impact cratering: A geologic process*. New York: Oxford University Press.

Michael G. G. 2013. Planetary surface dating from crater size–frequency distribution measurements: Multiple resurfacing episodes and differential isochron fitting. *Icarus* 226:885–890.

Michael G. G., Kneissl T., and Neesemann A. 2016. Planetary surface dating from crater size-frequency distribution measurements: Poisson timing analysis. *Icarus* 277:279–285.

Miller B. P. 1965. Distribution of small lunar craters based on Ranger 7 photographs. *Journal of Geophysical Research* 70:2265–2266.

Minton D. A. and Fassett C. I. 2016. Crater equilibrium as an anomalous diffusion process (abstract #2623). 47th Lunar and Planetary Science Conference. CD-ROM.

Mischna M. A., Richardson M. I., Wilson R. J., and McCleese D. J. 2003. On the orbital forcing of Martian

water and CO_2 cycles: A general circulation model study with simplified volatile schemes. *Journal of Geophysical Research Planets* 108:5062.

Montanari A., Asaro F., Michel H. V., and Kennett J. P. 1993. Iridium anomalies of late Eocene age at Massignano (Italy), and ODP Site 689B (Maud Rise, Antarctic). *Palaios* 8:420–437.

Montmessin F. 2006. The orbital forcing of climate changes on Mars. *Space Science Reviews* 125:457–472.

Moore H. J., Boyce J. M., and Hahn D. A. 1980. Small impact craters in the lunar regolith—Their morphologies, relative ages, and rates of formation. *Moon Planets* 23:231–252.

Moore J. M., McKinnon W. B., Spencer J. R., Howard A. D., Schenk P. M., Beyer R. A., Nimmo F., Singer K. N., Umurhan O. M., White O. L., Stern S. A., Ennico K., Olkin C. B., Weaver H. A., Young L. A., Binzel R. P., Buie M. W., Buratti B. J., Cheng A. F., Cruikshank D. P., Grundy W. M., Linscott I. R., Reitsema H. J., Reuter D. C., Showalter M. R., Bray V. J., Chavez C. L., Howett C. J. A., Lauer T. R., Lisse C. M., Parker A. H., Porter S. B., Robbins S. J., Runyon K., Stryk T., Throop H. B., Tsang C. C. C., Verbiscer A. J., Zangari A. M., Chaikin A. L., Wilhelms D. E., and the New Horizons Science Team 2016. The geology of Pluto and Charon through the eyes of New Horizons. *Science* 351:1284–1293.

Muller R. A., Becker T. A., Culler T. S., and Renne P. R. 2001. Solar system impact rates measured from lunar spherule ages. In *Accretion of extraterrestrial matter throughout Earth's history*, edited by Peucker-Ehrenbrink B. and Schmitz B. New York: Kluwer Academic/Plenum Publishers. pp. 447–462.

Murray J. B., Muller J.-P., Neukum G., Werner S. C., van Gasselt S., Hauber E., Markiewicz W. J., Head J. W. III, Foing B. H., Page D., Mitchell K. L., Portyankina G., and The HRSC Co-Investigator Team. 2005. Evidence from the Mars Express High Resolution Stereo Camera for a frozen sea close to Mars' equator. *Nature* 434:352–356.

Mustard J. F., Cooper C. D., and Rifkin M. K. 2001. Evidence for recent climate change on Mars from the identification of youthful near-surface ground ice. *Nature* 412:411–414.

Neukum G. 1983. Meteorite bombardment and dating of planetary surfaces. Translation of: Meteoritenbombardement und Datierung planetarer Oberflächen, Tenure Thesis, Ludwig-Maximilians University, Munich, Germany, NASA Technical Memorandum TM-77558, 1–186.

Neukum G. and Horn P. 1976. Effects of lava flows on lunar crater populations. *The Moon* 15:205–222.

Neukum G. and Ivanov B. A. 1994. Crater size distributions and impact probabilities on Earth from lunar, terrestrial-planet and asteroid cratering data. In *Hazards due to comets and asteroids*, edited by Gehrels T. Tucson, Arizona: The University of Arizona Press. pp. 359–416.

Neukum G. and Wise D. 1976. Mars: A standard crater curve and possible new time scale. *Science* 194:1381–1387.

Neukum G., König B., and Arkani-Hamed J. 1975. A study of lunar impact crater size-distributions. *The Moon* 12:201–229.

Neukum G., Ivanov B. A., and Hartmann W. K. 2001. Cratering records in the inner solar system in relation to the lunar reference system. *Space Science Reviews* 96:55–86.

Newsom H. E., Mangold N., Kah L. C., Williams J. M., Arvidson R. E., Stein N., Ollila A. M., Bridges J. C., Schwenzer S. P., King P. L., Granti J. A., Pinet P., Bridges N. T., Calef F., Wiens R. C., Spray J. G., Vaniman D. T., Elston W. E., Berger J. A., Garvin J. B., Palucis M. C., and the MSL Science Team 2015. Gale crater and impact processes—Curiosity's first 364 sols on Mars. *Icarus* 249:108–128.

Neish C. D. and Lorenz R. D. 2012. Titan's global crater population: A new assessment. *Planetary and Space Science* 60:26–33.

Nyquist L. E. and Shih C.-Y. 1992. The isotopic record of lunar volcanism. *Geochimica et Cosmochimica Acta* 56:2213–2234.

Nyquist L. E., Bogard D. D., and Shih C.-Y. 2001. Radiometric chronology of Moon and Mars. In *The century of space science*, edited by Bleeker J. A., Geiss J., and Huber M. Dordrecht, the Netherlands: Kluwer Publishers. pp. 1325–1376.

Oberbeck V. R. and Morrison R. H. 1974. Laboratory simulation of the herring bone pattern associated with lunar secondary crater chains. *Moon* 9:415–455.

O'Brien D. P. and Greenberg R. 2003. Steady-state size distributions for collisional populations: Analytical solution with size-dependent strength. *Icarus* 164:334–345.

O'Brien D. P. and Greenberg R. 2005. The collisional and dynamical evolutions of the main-belt and NEA size distributions. *Icarus* 178:179–212.

Ong L., Berger A. J., and Melosh H. J. 2011. Characterization of a Corinto crater ray on Mars (abstract #1552). 42nd Lunar and Planetary Science Conference. CD-ROM.

Öpik E. J. 1960. The lunar surface as an impact counter. *Monthly Notices of the Royal Astronomical Society* 120:404–411.

Öpik E. J. 1965. Mariner IV and craters on Mars. *Irish Astronomical Journal* 7:92–104.

Öpik E. J. 1966. The Martian surface. *Science* 153:255–265.

Ostrach L. R., Robinson M. S., Denevi B. W., and Thomas P. C. 2011. Effects of incidence angle on crater counting observations (abstract #1202). 42nd Lunar and Planetary Science Conference. CD-ROM.

Page D. P., Balme M. R., and Grady M. M. 2009. Dating Martian climate change. *Icarus* 203:376–389.

Papike J. J., Ryder G., and Shearer C. K. 1998. Lunar samples. In *Planetary materials*, edited by Papike J. J. Reviews in Minerology, vol. 36. Washington, D.C.: Mineralogical Society of America. pp. 5-1–5-234.

Pasckert J. H., Hiesinger H., and van der Bogert C. H. 2015. Small-scale lunar farside volcanism. *Icarus* 257:336–354.

Phillips R. J., Raubertas R. F., Arvidson R. E., Sarkar I. C., Herrick R. R., Izenberg N., and Grimm R. E. 1992. Impact craters and Venus resurfacing history. *Journal of Geophysical Research Planets* 97:15,923–15,948.

Phillips R. J., Davis B. J., Tanaka K. L., Byrne S., Mellon M. T., Putzig N. E., Haberle R. M., Kahre M. A., Campbell B. A., Carter L. M., Smith I. B., Holt J. W., Smrekar S. E., Nunes D. C., Plaut J. J., Egan A. F., Titus T. N., and Seu R. 2011. Massive CO_2 ice deposits sequestered in the south polar layered deposits of Mars. *Science* 332:838–841.

Pike R. J. 1974. Depth/diameter relations of fresh lunar craters: Revision from spacecraft data. *Geophysical Research Letters* 1:291–294.

Pike R. J. 1977. Apparent depth/apparent diameter relation for lunar craters. Proceedings, 8th Lunar Science Conference. pp. 3427–3436.

Pike R. J. and Wilhelms D. E. 1978. Secondary impact craters on the Moon: Topographic form and geologic process. Proceedings, 9th Lunar and Planetary Science Conference. pp. 907–909.

Platz T., Michael G. G., and Neukum G. 2010. Confident thickness estimates for planetary surface deposits from concealed crater populations. *Earth and Planetary Science Letters* 293:388–395.

Platz T., Michael G. G., Tanaka K. L., Skinner J. A. Jr., , Kneissl T., and Fortezzo C. M. 2013. Crater-based dating of geological units on Mars: Methods and application for the new global geological map. *Icarus* 225:806–827.

Plescia J. B. 2012. Uncertainties in the < 3 Ga lunar impact cratering chronology (abstract #1614). 43rd Lunar and Planetary Science Conference. CD-ROM.

Plescia J. B. 2015. Lunar crater forms on melt sheets—Origins and implications for self-secondary cratering and chronology (abstract #2054). 46th Lunar and Planetary Science Conference. CD-ROM.

Plescia J. B. and Robinson M. S. 2011. New constraints on the absolute lunar crater chronology (abstract #1839). 42nd Lunar and Planetary Science Conference. CD-ROM.

Plescia J. B. and Robinson M. S. 2015. Lunar self-secondary cratering: Implications for cratering and chronology (abstract #2535). 46th Lunar and Planetary Science Conference. CD-ROM.

Plescia J. B., Robinson M. S., and Paige D. A. 2010. Giordano Bruno: The young and the restless (abstract #2038). 41st Lunar and Planetary Science Conference. CD-ROM.

Popova O. P., Sidneva S. N., Shuvalov V. V., and Strelkov A. S. 2000. Screening of meteoroids by ablation vapor in high-velocity meteors. *Earth, Moon, and Planets* 82–83:109–128.

Popova O., Nemtchinov I., and Hartmann W. K. 2003. Bolides in the present and past Martian atmosphere and effects on cratering processes. *Meteoritics & Planetary Science* 38:905–925.

Popova O., Borovička J., Hartmann K., Spurný P., Gnos E., Nemtchinov I., and Trigo-Rodríguez J. M. 2011. Very low strengths of interplanetary meteoroids and small asteroids. *Meteoritics & Planetary Sciences* 46:1525–1550.

Pravec P. and Harris A. W. 2000. Fast and slow rotation of asteroids. *Icarus* 148:12–20.

Preblich B. S., McEwen A. S., and Studer D. M. 2007. Mapping rays and secondary craters from the Martian crater Zunil. *Journal of Geophysical Research Planets* 112: E05006.

Qiao L., Head J., Wilson L., Xiao L., Kreslavsky M., and Dufek J. 2017. Ina pit crater on the Moon: Extrusion of waning-stage lava lake magmatic foam results in extremely young crater retention ages. *Geology* 45:455–458.

Quantin C., Mangold N., Hartmann W. K., and Allemand P. 2007. Possible long-term decline in impact rates 1. Martian geological data. *Icarus* 186:1–10.

Quantin C., Popova O., Hartmann W. K., and Werner S. C. 2016. Young Martian crater Gratteri and its secondary craters. *Journal of Geophysical Research Planets* 121:1–23. https://doi.org/10.1002/2015JE004864.

Rampino M. R. and Caldeira K. 2015. Periodic impact cratering andextinction events over the last 260 million years. *Monthly Notices of the Royal Astronomical Society* 454:3480–3484.

ReVelle D. O. 1997. Historical detection of atmospheric impacts by large bolides using acoustic-gravity waves. *Annals of the New York Academy of Science* 822:284–302.

Robbins S. J. 2014. New crater calibrations for the lunar crater-age chronology. *Earth and Planetary Science Letters* 403:188–198.

Robbins S. J. and Hynek B. M. 2012. A new global database of Mars impact craters $\geq$1 km: 1. Database creation, properties, and parameters. *Journal of Geophysical Research Planets*, 117:E05004.

Robbins S. J. and Hynek B. M. 2014. The secondary crater population of Mars. *Earth and Planetary Science Letters* 400:66–76.

Robbins S. J., Antonenko I., Kirchoff M. R., Chapman C. R., Fassett C. I., Herrick R. R., Singer K., Zanetti M., Lehan C., Huang D., and Gay P. L. 2014. The variability of crater identification among expert and community crater analysts. *Icarus* 234:109–131.

Robbins S. J., Bierhaus E. B., and Dones L. H. 2015. Craters of the Saturnian satellite system: II. Mimas and Rhea (abstract #1654). 46th Lunar and Planetary Science Conference. CD-ROM.

Robbins S. J., Singer K. N., and Bray V. J., Schenk P., Lauer T. R., Weaver H. A., Runyon K., McKinnon W. B., Beyer R. A., Porter S., White O. L., Hofgartner J. D., Zangari A. M., Moore J. M., Young L. A., Spencer J. R., Binzel R. P., Buie M. W., Buratti B. J., Cheng A. F., Grundy W. M., Linscott I. R., Reitsema H. J., Reuter D. C., Showalter M. R., Tyler G. L., Olkin C. B., Ennico K. S., and Stern S. A., the New Horizons LORRI, MVIC Instrument Teams 2017a. Craters of the Pluto-Charon system. *Icarus* 287:187–206.

Robbins S. J., Riggs J., Weaver B. P., Bierhaus E. B., Chapman C. R., Kirchoff M. R., Singer K. N., and Gaddis L. R. 2017b. Revised recommended methods for analyzing crater size-frequency distributions. *Meteoritics & Planetary Sciences*. Forthcoming.

Roberts W. A. 1964. Secondary craters. *Icarus* 3:348–364.

Robinson M. S., Brylow S. M., Tschimmel M., Humm D., Lawrence S. J., Thomas P. C., Denevi B. W., Bowman-Cisneros E., Zerr J., Ravine M. A., Caplinger M. A., Ghaemi F. T., Schaffner J. A., Malin M. C., Mahanti P., Bartels A., Anderson J., Tran T. N., Eliason E. M., McEwen A. S., Turtle E., Jolliff B. L., and Hiesinger H. 2010. Lunar Reconnaissance Orbiter Camera (LROC) instrument overview. *Space Science Reviews* 150:81–124.

Robinson M. S., Boyd A. K., Denevi B. W., Lawrence S. J., McEwen A. S., Moser D. E., Povilaitis R. Z., Stelling R. W., Suggs R. M., Thompson S. D., and Wagner R. V. 2015. New crater on the Moon and a swarm of secondaries. *Icarus* 252:229–235.

Robinson M. S., Thomas P. C., Plescia J. B., Denevi B. W., Burns K. N., Bowman-Cisneros E., Henriksen M. R., van der Bogert C. H., Hiesinger H., Mahanti P., Stelling R. W., and Povilaitis R. Z. 2016. An exceptional grouping of lunar highland smooth plains: Geography, morphology, and possible origins. *Icarus* 273:121–134.

Ross H. P. 1968. A simplified mathematical model for lunar crater erosion. *Journal of Geophysical Research* 73:1343–1354.

Russell C. T., Raymond C. A., Coradini A., McSween H. Y., Zuber M. T., Nathues A., De Sanctis M. C., Jaumann R., Konopliv A. S., Preusker F., Asmar S. W., Park R. S., Gaskell R., Keller H. U., Mottola S., Roatsch T., Scully J.

E. C., Smith D. E., Tricarico P., Toplis M. J., Christensen U. R., Feldman W. C., Lawrence D. J., McCoy T. J., Prettyman T. H., Reedy R. C., Sykes M. E., and Titus T. N. 2012. Dawn at Vesta: Testing the protoplanetary paradigm. *Science* 336:684–686.

Schaber G. G., Strom R. G., Moore H. J., Soderblom L. A., Kirk R. L., Chadwick D. J., Dawson D. D., Gaddis L. R., Boyce J. M., and Russel J. 1992. Geology and distribution of impact craters on Venus: What are they telling us? *Journal of Geophysical Research Planets* 97:13,257–13,301.

Schenk P., Hoogenboom T., and Kirchoff M. 2017. Auto-secondaries on a midsize icy moon: Bright rayed crater Inktomi (Rhea) (abstract #2686). 48th Lunar and Planetary Science Conference. CD-ROM.

Schmedemann N., Kneissl T., Ivanov B. A., Michael G. G., Wagner R. J., Neukum G., Ruesch O., Hiesinger H., Krohn K., Roatsch T., Preusker F., Sierks H., Jaumann R., Reddy V., Nathues A., Walter S. H. G., Neesemann A., Raymond C. A., and Russell C. T. 2014. The cratering record, chronology and surface ages of (4) Vesta in comparison to smaller asteroids and the ages of HED meteorites. *Planetary and Space Science* 103:104–130.

Schmitz B. 2013. Extraterrestrial spinels and the astronomical perspective on Earth's geological record and evolution of life. *Chemie der Erde* 73:117–145.

Schmitz B., Peucker-Ehrenbrink B., Lindström M., and Tassinari M. 1997. Accretion rates of meteorites and extraterrestrial dust in the Early Ordovician. *Science* 278:88–90.

Schmitz B., Tassinari M., and Peucker-Ehrenbrink B. 2001. A rain of ordinary chondritic meteorites in the early Ordovician. *Earth and Planetary Science Letters* 194:1–15.

Schmitz B., Boschi S., Cronholm A., Heck P. R., Monechi S., Montanari A., and Terfelt F. 2015. Fragments of Late Eocene Earth-impacting asteroids linked to disturbance of asteroid belt. *Earth and Planetary Science Letters* 425:77–83.

Schultz P. H. 1992. Atmospheric effects on ejecta emplacement and crater formation on Venus from Magellan. *Journal of Geophysical Research Planets* 97:16,183–16,248.

Schultz P. H. and Spencer J. 1979. Effects of substrate strength on crater statistics: Implications for surface ages and gravity scaling. Proccedings, 10th Lunar and Planetary Science Conference. pp. 1081–1083.

Schultz P. H., Gault D., and Greeley R. 1977. Interpreting statistics of small lunar craters. Proceedings, 8th Lunar Science Conference. pp. 3539–3564.

Seiff A. 1983. Thermal structure of the atmosphere of Venus. In *Venus*, edited by Hunten D. M., Colin L., Donahue T. M., and Moroz V. I. Tucson, Arizona: The University of Arizona Press. pp. 215–279.

Seiff A. and Kirk D. B. 1977. Structure of the atmosphere of Mars in summer at mid-latitudes. *Journal of Geophysical Research* 82:4364–4378.

Shoemaker E. M. 1960. Ballistics of the Copernican ray system. *Proceedings of the Lunar and Planetary Exploration Colloquium* 2:7–21.

Shoemaker E. M. 1962. Interpretation of lunar craters. In *Physics and astronomy of the Moon*, edited by Kopal Z. New York: Academic Press. pp. 283–359.

Shoemaker E. M. 1965. Preliminary analysis of the fine structure of the lunar surface in Mare Cognitum. In *The nature of the lunar surface*, edited by Heiss W. N., Menzel D. R., and O'Keefe J. A. Baltimore, Maryland: Johns Hopkins University Press. pp. 23–77.

Shoemaker E. M. 1998. Long-term variations in the impact cratering rate on Earth. *Geological Society, London, Special Publications* 140:7–10.

Shoemaker E. M. and Wolfe R. E. 1986. Mass extinction, crater ages and comet showers. In *The galaxy and the solar system*, edited by Smoluchowski R., Bahcall J. N., and Matthews W. S. Tucson, Arizona: The University of Arizona Press. pp. 338–386.

Shoemaker E. M., Hackman R. J., and Eggleton R. E. 1963. Interplanetary correlation of geologic time. *Advances in the Astronautical Sciences* 8:70–89.

Shoemaker E. M., Batson R. M., Holt H. E., Morris E. C., Rennilson J. J., and Whitaker E. A. 1968. III. Television observations from Surveyor VII. In *Surveyor 7 mission report. Part 2—Science results*. JPL Technical Report 32-1264, pp.9–76.

Shoemaker E. M., Batson R. M., Bean A. L., Conrad C. Jr., Dahlem D. H., Goddard E. N., Hait M. H., Larson K. B., Schaber G. G., Schleicher D. L., Sutton R. L., Swann G. A., and Waters A. C. 1970. Preliminary geologic investigation of the Apollo 12 landing site: Part A: Geology of the Apollo 12 Landing Site. In *Apollo 12 Preliminary Science Report*. Washington, D.C.: NASA. pp. 113–156.

Silber E. A., ReVelle D. O., Brown P. G., and Edwards W. N. 2009. An estimate of the terrestrial influx of large meteoroids from infrasonic measurements. *Journal of Geophysical Research Planets* 114:E08006.

Smith M. R., Gillespie A. R., and Montgomery D. R. 2008. Effect of obliteration on crater-count chronologies for Martian surfaces. *Geophysical Research Letters* 35:L10202.

Snyder G. A., Borg L. E., Nyquist L. E., and Taylor L. A. 2000. Chronology and isotopic constraints on lunar evolution. In *The origin of the Earth and the Moon*. Tucson, Arizona: The University of Arizona Press. pp. 361–395.

Soderblom L. A. 1970. A model for small-impact erosion applied to the lunar surface. *Journal of Geophysical Research* 75:2655–2661.

Soderblom L. A., Condit C. D., West R. A., Herman B. M., and Kreidler T. J. 1974. Martian planetwide crater distributions: Implications for geologic history and surface processes. *Icarus* 22:239–263.

Soto A., Mischna M., Schneider T., Lee C., and Richardson M. 2015. Martian atmospheric collapse: Idealized GCM studies. *Icarus* 250:553–569.

Souness C., Hubbard B., Milliken R. E., and Quincey D. 2012. An inventory and population-scale analysis of Martian glacier-like forms. *Icarus* 217:243–255.

Speyerer E. J., Povilaitis R. Z., Robinson M. S., Thomas P. C., and Wagner R. V. 2016. Quantifying crater production and regolith overturn on the Moon with temporal imaging. *Nature* 538:215–218.

Stöffler D. and Ryder G. 2001. Stratigraphy and isotope ages of Lunar geologic units: Chronological standard for the inner solar system. *Space Science Reviews* 96:9–54.

Stöffler D., Ryder G., Ivanov B. A., Artemieva N. A., Cintala M. J., and Grieve R. A. F. 2006. Cratering history and lunar chronology. *Reviews in Mineralogy and Geochemistry* 60:519–596.

Strom R. G. and Fielder G. 1968a. Multiphase development of the lunar crater Tycho. *Nature* 217:611–615.

Strom R. G. and Fielder G. 1968b. Multiphase eruptions associated with the lunar craters Tycho and Aristarchus. *Communications of the Lunar and Planetary Laboratory* 8:235–288.

Strom R. G., Chapman C. R., Merline W. J., Solomon S. J., and Head J. W. III. 2008. Mercury cratering record viewed from MESSENGER's first flyby. *Science* 321:79–81.

Strom R. G., Banks M. E., Chapman C. R., Fassett C. I., Forde J. A., Head J. W. III, Merline W. J., Prockter L. M., and Solomon S. C. 2011. Mercury crater statistics from MESSENGER flybys: Implications for stratigraphy and resurfacing history. *Planetary and Space Science* 59:1960–1967.

Suggs R. M., Moser D. E., Cooke W. J., and Suggs R. J. 2014. The flux of kilogram-sized meteoroids from lunar impact monitoring. *Icarus* 238:23–36.

Swindle T. D., Kring D. A., and Weirich J. R. 2014. 40Ar/39Ar ages of impacts involving ordinary chondrite meteorites. *Geological Society, London, Special Publication* 378:333–347.

Thorslund P., Wickman F. E., and Nyström J. O. 1984. The Ordovician chondrite from Brunflo, central Sweden. I. General description and primary minerals. *Lithos* 17:87–100.

Toon O. B., Pollack J. B., Ward W., Burns J. A., and Bilski K. 1980. The astronomical theory of climatic change on Mars. *Icarus* 44:552–607.

Tornabene L. L., Moersch J. E, McSween H. Y. Jr., McEwen A. S., Piatek J. L., Milam K. A., and Christensen P. R. 2006. Identification of large (2–10 km) rayed craters on Mars in THEMIS thermal infrared images: Implications for possible Martian meteorite source regions. *Journal of Geophysical Research Planets* 111:E10006.

Trask N. J. 1966. Size and spatial distribution of craters estimated from the Ranger photographs. In *Ranger VIII and IX, Part II, Experimenters' analyses and interpretations*. California Institute of Technology, Jet Propulsion Laboratory Technical Report 32-800. pp. 252–264.

Turner G. 1977. Potassium-argon chronology of the Moon. *Physics and Chemistry of the Earth* 10:145–195.

Van der Bogert C. H., Hiesinger H., McEwen A. S., Dundas C., Bray V., Robinson M. S., Plescia J. B., Reiss D., Klemm K. and the LROC Team 2010. Discrepancies between crater size-frequency distributions on ejecta and impact melt pools at lunar craters: An effect of differing target properties? (abstract #2165) 41st Lunar and Planetary Science Conference. CD-ROM.

Van der Bogert C. H., Michael G., Kneissl T., Hiesinger H., and Pasckert J. H. 2015a. Effects of count area size on absolute model ages derived from random crater size-frequency distributions (abstract #1742). 46th Lunar and Planetary Science Conference. CD-ROM.

Van der Bogert C. H., Michael G., Kneissl T., Hiesinger H., and Pasckert J. H. 2015b. Development of guidelines for recommended lunar CSFD count area sizes via analysis of random CSFDs (abstract #9023). Workshop on Issues in Crater Studies and the Dating of Planetary Surfaces.

Van der Bogert C. H., Gaddis L., Hiesinger H., Ivanov M., Jolliff B., Mahanti P., and Pasckert J. H. 2016. Revisiting the CSFDs of the Taurus Littrow dark mantle deposit: Implications for age determinations of pyroclastic deposits (abstract #1616). 47th Lunar and Planetary Science Conference. CD-ROM.

Van der Bogert C. H., Hiesinger H., Dundas C. M., Krüger T., McEwen A. S., Zanetti M., and Robinson M. S. 2017. Origin of discrepancies between crater size-frequency distributions of coeval lunar geologic units via target property contrasts. *Icarus*. https://doi.org/10.1016/j.icarus.2016.11.040

Vasavada A. R., Milavec T. J., and Paige D. A. 1993. Microcraters on Mars: Evidence for past climate variations. *Journal of Geophysical Research Planets* 98:3469–3476.

Ward W. R., Murray B. C., and Malin M. C. 1974. Climate variations on Mars: 2. Evolution of carbon dioxide atmosphere and polar caps. *Journal of Geophysical Research* 79:3387–3395.

Warner N. H., Gupta S., Calef F., Grindrod P., Boll N., and Goddard K. 2015. Minimum effective area for high resolution crater counting of Martian terrains. *Icarus* 245:198–240.

Werner S. C., Ivanov B. A., and Neukum G. 2009. Theoretical analysis of secondary cratering on Mars and an image-based study on the Cerberus Plains. *Icarus* 200:406–417.

Wieler R. and Graf T. 2001. Cosmic ray exposure history of meteorites. In *Accretion of extraterrestrial matter throughout Earth's history*, edited by Peucker-Ehrenbrink B. and Schmitz B. New York: Kluwer Academic. pp. 221–240.

Wilcox B. B., Robinson M. S., Thomas P. C., and Hawke B. R. 2005. Constraints on the depth and variability of the lunar regolith. *Meteoritics & Planetary Science* 40:695–710.

Williams J.-P., Pathare A. V., and Aharonson O. 2014a. The production of small primary craters on Mars and the Moon. *Icarus* 235:23–36.

Williams J.-P., Paige D. A., Plescia J. B., Pathare A. V., and Robinson M. S. 2014b. Crater size-frequency distribution on the ejecta of Giordano Bruno (abstract #2882). 45th Lunar and Planetary Science Conference. CD-ROM.

Williams J.-P., Bandfield J. L., Paige D. A., Greenhagen B. T., Speyerer E. J., and Ghent R. R. 2016a. A recent, large multi-impact event on the Moon (abstract #2637). 48th Lunar and Planetary Science Conference. CD-ROM.

Williams J.-P., Sefton-Nash E., and Paige D. A. 2016b. The temperatures of Giordano Bruno crater observed by the Diviner Lunar Radiometer Experiment: Application of an effective field of view model for a point-based data set. *Icarus* 273:205–213.

Wittenberg L. J., Cameron E. N., Kulcinski G. L., Ott S. H., Santarius J. F., Sviatoslavsky G. I., Sviatoslavsky I. N., and Thompson H. E. 1992. A review of helium-3 resources and acquisition for use as fusion fuel. *Fusion Technology* 21:2230–2253.

Wood C. A., Lorenz R., Kirk R., Lopes R., Mitchell K., and Stofan E. 2010. Impact craters on Titan. *Icarus* 206:334–344.

Wünnemann K., Nowka D., Collins G. S., Elbeshausen D., and Bierhaus M. 2010. Scaling of impact crater formation on planetary surfaces—Insights from numerical modeling. In *Proceedings of the 11th Hypervelocity Impact Symposium*, edited by Hiemaier S. Freiburg, Germany: Fraunhofer. pp. 1–16.

Xiao Z. and Strom R. G. 2012. Problems determining relative and absolute ages using the small crater population. *Icarus* 220:254–267.

Xiao Z., Prieur N. C., and Werner S. C. 2016. The self-secondary crater population of the Hokusai crater on

Mercury. *Geophysical Research Letters*, https://doi.org/10.1002/2016GL069868.

Yelle R. V., Strobel D. F., Lellouch E., and Gautier D. 1997. Engineering models for Titan's atmosphere. *HUYGENS Science, Payload and Mission, ESA SP* 1177:243–256.

Young R. A. 1975. Mare crater size-frequency distributions: Implications for relative surface ages and regolith development. Proceedings, 6th Lunar Science Conference. pp. 2645–2662.

Zahnle K., Schenk P., Levison H., and Dones L. 2003. Cratering rates in the outer solar system. *Icarus* 163:263–289.

Zahnle K., Alvarellos J. L., Dobrovolskis A., and Hamill P. 2008. Secondary and sesquinary craters on Europa. *Icarus* 194:660–674.

Zanetti M., Jolliff B., van der Bogert C. H., and Hiesinger H. 2012. Equal-area radial crater counts at large Copernican impact craters: Implications for late-stage ejecta emplacement? (abstract #2131). 43rd Lunar and Planetary Science Conference. CD-ROM.

Zanetti M., Stadermann A., Jolliff B., Hiesinger H., van der Bogert C. H., and Plescia J. 2017. Evidence for self-secondary cratering of Copernican-age continuous ejecta deposits on the Moon. *Icarus*. https://doi.org/10.1016/j.icarus.2017.01.030

Zellner N. E. B. and Delano J. W. 2015. $^{40}Ar/^{39}Ar$ ages of lunar impact glasses: Relationships among Ar diffusivity, chemical composition, shape, and size. *Geochimica et Cosmochimica Acta* 161:203–218.